Investigating local adaptation in the wood-decay fungus *Trichaptum abietinum* through common garden experiments and population genomics

Ine-Susanne Hopland Methlie

Master of Science thesis (60 credits)

Section for Genetics and Evolutionary Biology
Department of Biosciences
Faculty of Mathematics and Natural Sciences

University of Oslo

June / 2021

2021

Investigating local adaptation in the wood-decay fungus *Trichaptum abietinum* through common garden experiments and population genomics

Author – Ine-Susanne H. Methlie

http://www.duo.uio.no/

Trykk: Reprosentralen, Universitetet i Oslo

Acknowledgements

First, I would like to thank my wonderful supervisors: Inger, Håvard, Dabao and Peris.
Inger, thank you so much for your valuable guidance, for always finding time for me and for your positive energy that makes it a dream to be a master student. Håvard, thank you for your good advice and for your invaluable help in the writing process. Thank you Dabao for your immense patience and kindness. I appreciate you for always taking the time to help, for making even the most stupid questions seem smart and for our shared love for tea and snacks. Thank you, Peris, for your encouragement and for solving all my bioinformatic emergencies.

Thank you Malin for your help in the lab, our conversations outside the lab and for the great time we had in the field together with Inger.

Thank you to the Fungal Master's: Vilde, Sondre, Eivind + Markus and Erik, for being the best people and for our friendship! I don't think I would have spent as much time in the office as I have, if it wasn't for the fact that I love seeing all your faces every day and hang out in The Lounge. I would also like to thank everyone in the Oslo Mycology Group (OMG) for making this the best environment to be a master student.

To my girls, Ingrid, Jessica and Henninge; thank you for our friendship and for your invaluable support. I am inspired by all three of you every day. This journey would not have been the same without you.

Finally, I would like to thank my partner, Ask, for always being there for me and reminding me of a healthy work/life balance. Also, thank you for enduring my lengthy stories (including acted out scenes) from my everyday life, even though you could work a bit on your response as an audience.

Table of contents

Abstract

Rapid climatic changes already affect ecosystems all over the globe. *Trichaptum abietinum* has a wide geographic distribution covering large climatic gradients, which could indicate adaptation to local environments in different populations or high phenotypic plasticity within the species. How well populations are able to adapt to the local environment could predict how the species distribution will react to an altered climate. In this study, the process of local adaptation has been investigated in the fungal wood decay species *Trichaptum abietinum*.

Population genomic analyses coupled with common garden experiments have been used to investigate if different populations of *T. abietinum* have gone through adaptation to local climatic conditions, and to detect possible environmental drivers and genetic mechanisms that cause adaptation.

Clear population structure and divergence were detected between eastern and western populations, albeit little divergence was found within these two groups of *T. abietinum*. A Redundancy Analysis proposed adaptation towards a wet and stable, coastal climate in western specimens, and possibly towards high temperatures in a southern population. Common garden experiments, measuring decay and hyphal extension rate, indicated static trends between populations at different temperatures.

The observed divergence between eastern and western populations could be due to different immigration routes of *T. abietinum,* connected to two separate postglacial immigration histories of *Picea abies*. Another possibility is adaptation to the distinct conditions in eastern and western Norway. However, due to a clear population structure the results from the Redundancy Analysis performed could be misleading. Several genes, with known and unknown gene functions, was detected in areas of SNPs possibly under selection for high levels of precipitation and isothermality. Further studies, including additional sampling sites, larger sample sizes and more extensive genomic analysis, should be conducted to confirm the suggested patterns found in this study.

1 Introduction

The climate on earth is now changing at accelerating rates due to human activity (Pecl et al., 2017). The observed alterations in the 21st-century are the greatest global changes that have been observed in the past 65 million years (Kemp et al., 2015). These rapid changes are already resulting in a large-scale biological response, affecting ecosystems all over the world (Pecl et al., 2017). Environmental changes, due to climatic alterations, are likely to become an impelling factor for a future transformation of global biodiversity, and a redistribution of life on earth (Pecl et al., 2017).

There are mainly four possible outcomes for species when they are faced with abrupt environmental changes: Extinction, tolerance/plasticity, escape/dispersion or adaptation (Olson-Manning et al., 2012). When environmental alterations are extensive, and occurs at extreme rates, populations go extinct; they cannot adapt physiologically, and might not be able to move to a more favourable location. For instance, amphibian populations are in decline on a global scale (Gratwicke et al., 2016). The decreasing population numbers are hypothesized to be caused mainly by habitat loss or disruption, caused by alterations in climate and human activity (Green, 1999; Stuart et al., 2004), in combination with outbreaks of fungal and viral pathogens (Green, 1999; Gratwicke et al., 2016).

However, many species are able to avoid extinction due to a high ability of tolerance, or phenotypic plasticity, to varied environmental circumstances. In the gras, *Phalaris arundinacea*, high plasticity is observed in both morphological and physiological traits, in response to differences in light, nitrogen soil content and moisture (Martina & von Ende, 2012). In Europe, a widening of annual fruiting season for several fungal species has been observed. These changes are thought to correlate with an extended plant growth season in Europe, as many of these fungi are growing in symbiosis with plants, possibly connected to climatic alterations (Kauserud et al., 2012).

Some populations handle unfavourable conditions by changing locations. This response depends on the innate capability of dispersal or relocation, which varies greatly between species. Palaeobotanical and genetic evidence for species migration over the last 25 000 years have concluded that species ranges have changed in close correlation with global climatic

cycles (Aitken et al., 2008). Records of pollen and analyses of cpDNA have shed light on the vast migration of several tree species, spreading from glacial refugia with the retreat of ice sheets following climatic warming (Davis & Shaw, 2001; Petit et al., 2004). Several fungal species have also shown a clear ability to migrate as a response to climatic changes. In a study on altitudinal changes in fungal fruiting, it was found that many fungal species were fruiting at significantly higher elevations in alpine areas in 2010 than what was observed in 1960, possibly as a response to a shift in climate (Diez et al., 2020). However, many species, including fungal species, are unable of long-distance migration or dispersal over large areas. In ectomycorrhizal fungi, successful dispersal has been observed to decrease rapidly with increasing distances, ranging from only 1 to 5 km, from spore sources (Peay et al., 2012). In Galante et al (2011), basidiospore dispersal of six different ectomycorrhizal species showed that 95% of spores were predicted to fall within 1 meter of the spore producing cap.

If species are incapable of having a plastic response or relocate, a last option to avoid extinction would be to adapt (Hoffmann & Sgrò, 2011). Local adaptation is a mode of selection that enables species or populations to evolve as a response to specific environmental conditions (Williams, 1996). The ability of a species to adapt depends on the genetic variation that is already present in the pangenome of a species, phenotypic plasticity, mutation rate, competition, biotic interactions and selection pressure opposed from the environment (Aitken et al., 2008; Ohlson et al., 2011). Research on local adaptation has been vastly explored in plants (Clausen et al., 1941; Kronholm et al., 2012) while the mechanisms behind local adaptation in many other organism groups remain unexplored.

There are several approaches to study the aspect of local adaptation in organisms: Genome analysis can reveal genomic differences between populations, caused by diverging selection for variants advantageous to specific environmental conditions. This has been demonstrated in wild species of the model plant *Arabidopsis* (Kubota et al. 2015) and in populations of the fungal species *Neurospora crassa* (Ellison et al., 2011), where specific genetic locations involved in local adaptation to climatic conditions was discovered. Common garden experiments can show how different populations react phenotypically to identical conditions, where divergent responses may suggest local adaptation among populations. This has been done on insect species *Fomica selysi* (Purcell et al., 2016) or in several different fungal species (Ellison et al., 2011; Maynard et al., 2019) connecting environmental gradients to different phenotypic or genetic traits.

Fungi have a great impact on all terrestrial ecosystems (Galante et al., 2011), but very little is known about local adaptation and processes behind broad scale biogeographical patterns in different species (Maynard et al., 2019). Saprotrophic fungi have an important role in forest ecosystems, where they decompose dead organic material and recycle nutrients back into the environment (Treseder & Lennon, 2015). This process affects the global carbon and nutrient dynamics (Maynard et al, 2019). Consequently, it is crucial to gain more insight on how fungal saprotrophic species adapt to their environments to be able to model a future redistribution of populations that could accompany current, and predicted shifts in climate.

Climatic conditions have been shown to have a large impact on populations of fungi. Genetic differentiation among populations of *Suillus brevipes*, an ectomycorrhizal species living with the roots of pine trees, was found across North America (Branco et al., 2017). The populations are thought to be adapted to varying levels of temperature and precipitation differentiating between locations (Branco et al., 2017). Two cryptic and recently diverged populations were found in *Neurospora crassa*, revealing chromosomal regions of extreme divergence, containing specific genes possibly involved in cold response (Ellison et al., 2011). Several species of saprotrophic fungi have demonstrated a fundamental trade-off between stress tolerance and competitive ability, making genotypes specifically adapted to local climatic conditions (Maynard et al, 2019). It is proposed that the effects of climate, pared with edaphic characteristics, are the main drivers for the distribution of fungi at a local scale (Maynard et al, 2019).

The focal species in this study, *Trichaptum abietinum*, is a saprotrophic wood decay fungus belonging to the class of Agaricomycetes in the order Hymenochaetales. *Trichaptum abietinum* is abundant all over the northern hemisphere (Seierstad et al., 2021). In Norway, the species is present in a broad range of climatic zones in all parts of the country, where it grows on recently fallen dead coniferous wood, mainly *Picea abies* (Kauserud & Schumacher, 2003). The species can easily be brought into the lab, and cultured *in vitro* as demonstrated in previous studies (Kauserud & Schumacher, 2003).

The main aim of this study is to use population genomic analyses, coupled with common garden experiments, to investigate if different populations of *T. abietinum* in Norway has gone through

adaptation to local climatic conditions. Based on its widespread geographic distribution in Norway, I asked whether *T. abietinum* is a highly plastic species, or if different populations are adapted to local environments, enabling them to respond to varying climatic conditions. To answer this question, I have obtained isolates of *T. abietinum* from six different locations across South-Norway. Through population genomic analysis, mechanisms that may have contributed to adaptation was investigated by analysing genetic variation among the sampled populations, and by identifying and exploring genomic regions that may be correlated to climatic variables. Additionally, whether phenotypic variation exists between populations was examined by measuring decay and hyphal extension rate when exposed to different temperatures. These results can be used to further elucidate important mechanisms behind local adaptation in fungi and potentially predict how the future distribution of *T. abietinum* might change in relation to altered climatic conditions.

2 Materials and Methods

2.1 Sampling

Sporocarps of *T. abietinum* were collected from six localities in three different climate zones of southern Norway (Table 1). A total of ten individual fruit bodies were collected from each of the six locations. Fruit bodies were collected almost exclusively on dead *Picea abies* logs, while a few individuals also appeared on dead wood of *Pinus sylvestris*. The samples were dried in room temperature and stored dry in paper bags. Like many wood decaying fungi, the sporocarp can be stored dry for longer periods.

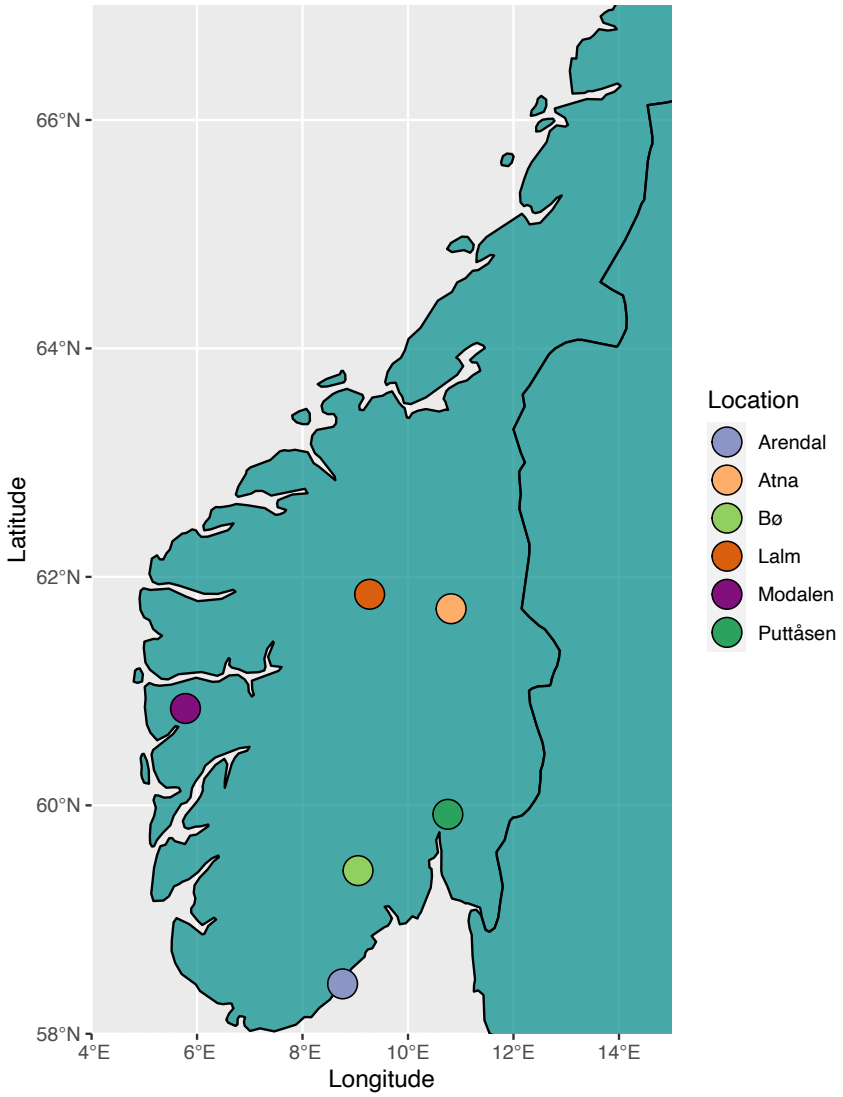

Figure 1: Map illustrating the six sampling locations in South-Norway color coded after the respective site. Ten fruit bodies of *Trichaptum abietinum* were sampled from each location during field work in September and October 2019.

2.2 Lab work

2.2.1 Culturing

Dried sporocarps may be revived, and continue to produce spores, after getting rewetted. For simplicity, haploid monokaryotic cultures was preferred for the whole genome sequencing approach. In order to make monokaryotic fungal cultures, each sampled fruit body was placed in a paper towel, and moistened with distilled water for 1-2 hours. To facilitate spore shooting a small piece of the fruit body was glued to the lid of a petri dish, using silicone grease from Merck Millipore (Darmstadt, Germany). The petri dishes contained 3% malt extract agar with 10 mg/L Tetracycline 100 mg/L Ampicillin, 25 mg/L Streptomycin and 1 mg/L benomyl (MEA+). These are substances well tolerated by basidiomycetes, but efficient in keeping ascomycetes and bacteria from contaminating the plate. The petri dishes were closed with parafilm and left in a dark incubator at 20 ℃. After 12-24 hours the fruit bodies had sporulated and single germinated spores were isolated and transferred to new plates of MEA+, using a sterile scalpel, and further kept on 20 ℃ in a dark incubator.

In order to control that only one spore was included, and the culture was in fact a monokaryotic culture and not a dikaryotic culture, a small sample of mycelia from each culture were prepared for microscopy after 2-3 weeks of growth, using Cotton blue (0.1%) to highlight the mycelial cells. *Trichaptum abietinum* possess clamps, visible structures between cells, that support the distribution nuclei across cells in dikaryotic mycelia (Krings et al., 2011). Clamp connections are a characteristic of Basidiomycetes (Krings et al., 2011), and makes it possible to distinguish between monokaryotic or dikaryotic mycelia on a microscopic level. This facilitates the process of isolating haploid monokaryotic cultures for sequencing, and for creating dikaryotic crosses of selected monokaryotic cultures. Each microscope slide was investigated on 400 x resolution to affirm the absence of clamps between septa and thus confirming haploid, monokaryotic cultures.

2.2.2 Species identification: PCR and Sanger sequencing

In order to confirm that the cultivated samples were *T. abietinum*, and not morphologically similar species or other contaminants, a PCR followed by Sanger Sequencing of the ITS region was performed. PCR was conducted using the Phire Plant Direct PCR Kit supplied by Thermo Scientific (Waltham, USA) using the following protocol: a small amount of mycelia (under 1 mg), was scraped from each culture using the tip of a 1250 μL pipette. The sampled mycelia were transferred to 1.5 mL Eppendorf tubes with 20 μL of dilution buffer (Phire Plant Direct PCR kit) and spun down. A master mix was prepared with 10 μL Phire Plant PCR Buffer, 2 μL of each primer, ITS1(5 μM) and ITS4 (5 μM) (White et al., 1990), 4.8 uL milliQ H2O, and 0.2 μL of Phire Hot start II DNA polymerase. After vortexing, 0.5 μL of diluted buffer with harvested mycelia was added. The PCR was performed in Eppendorf Mastercycler nexus GSX1 from Eppendorf AG (Hamburg Germany) on the following program: Initial denaturation on 98 ℃ for 5 minutes, followed by 40 cycles of denaturation on 98 ℃ for 5 seconds, annealing on 54 ℃ for 5 seconds, and extension on 72 ℃ for 20 seconds. After cycling, a final extension on 72℃ for 1 minute, and hold on 10 ℃ followed.

To purify the final PCR products, removing primers and dNTPs, an Exosap protocol was performed, using The Illustra ExoProStar 1-Step from GE healthcare (Chicago, USA). 2 μL of a 10% ExoSAP-it solution was added to each sample containing 5 μL PCR product, before an incubation step of 37 ℃ for 15 minutes, enzyme denaturation on 80 ℃ for 15 minutes and hold at 10 ℃.

The ITS amplicons were Sanger sequenced at Eurofins Scientific (Hamburg, Germany), with the ITS4 primer. Taxonomical identity was verified using BLAST (Altschul et al., 1990) on the National Centre of Biotechnology Information (NCBI) database (U.S National Library of Medicine).

2.2.3 DNA extraction and Illumina whole genome sequencing

To prepare samples for DNA isolation, a piece from each culture was transferred to a new MEA petri dish, this time without the use of antibiotics. Small pieces of each culture were placed to grow on sheets of nylon in new MEA petri dishes. This makes it easier to harvest mycelia later for DNA extraction without contaminating the samples with agar. DNA was extracted from

each culture, using the E.Z.N.A Fungal DNA kit (Omega Bio-Tek). The cultures were harvested after about four weeks of growth, where 25% of the mycelia on one plate was scraped off and transferred to 2 mL Lysing Matrix E tubes (MP, Biomedicals, Santa Ana, CA, USA) with 30 µL RNase (Qiagen, Hilden, Germany) and 600 µL CSPL Buffer (E.Z.N.A fungal DNA kit). The mycelium was crushed and homogenized in FastPrep-24 (MP Medicals, Santa Ana, CA, USA) for 2 x 20 seconds at 4.5 m/s^2. DNA extraction wad performed following the manufacturers protocol: Tubes were incubated at 65 ℃ for 30 minutes before cooling to room temperature and spun down. 600 µL of chloroform was added to each tube and vortexed. Tubes were centrifuged at 10 000 x g for 10 minutes and 450 mL of the upper layer was carefully transferred into new 1.5 mL tubes. 225 µL CXD buffer and 450 µL of 96% ethanol was added and tubes vortexed. A HiBind DNA mini column was inserted into a 2 mL collection tube. To equilibrate the column, 100 µL 3M NaOH was added and left for 4 minutes. Tubes were centrifuged at maximum speed for 20 seconds and filtrate discarded. The samples were transferred to the HiBind DNA mini columns and centrifuged at 10 000 x g for 1 minute, afterwards the HiBind DNA mini columns were inserted to new 2 mL collection tubes. Filtrate and collection tubes were discarded before 650 µL DNA washing buffer was added. Samples were centrifuged at 10 000 x g for 1 minute and filtrate discarded again. This last step was repeated for a second DNA wash buffer step. HiBind DNA mini column was transferred to a clean 1.5 mL microcentrifuge tube, 50 µL elution buffer heated to 65 ℃ added and tubes put on 65 ℃ incubator for 5 minutes. Tubes were centrifuged at maximum speed for 1 minute. Isolated DNA was assessed with Nanodrop, Qbit and Gel electrophoresis, to confirm the quality and concentration of DNA in each sample.

The DNA-Samples were sequenced with Illumina Whole Genome Sequencing at the Norwegian Sequencing Centre. Libraries were made by the Norwegian Sequencing Centre using 1 µL of genomic DNA, sheared using 96 microTUBE-50 AFA Fiber plates (Covaris Inc., Woburn, MA, USA) on a Covaris E220 system (Covaris Inc., Woburn, MA, USA). Target fragment size was 300-400 bp. gDNA samples were cleaned using a small volume Mosquito liquid handler (TTP Labtech), with 1:1 ratio Kapura Pure beads (Roche, Basel, Switzerland), eluted in Tris-CL with pH 8.0. Library preparations was done with 500 ng sheared DNA, using Kapa Hyper library prep kit (Roche, Basel, Switzerland). Barcodes were added with Illumina UD 96 Index kit (Roche, Basel, Switzerland), and standard library quality control with standard sensitivity NGS Fragment kit (Agilent, Santa Clara, CA, USA). Quantification was conducted

in a qPCR with Kapa Library quantification Kit (Roche, Base, Switzerland). 2 x 150 paired end Illumina read were generated. Some samples were sequenced with Illumina Hiseq 4000, and some were sequenced with Illumina Novaseq.

2.3 Bioinformatics

2.3.1 Processing of high throughput sequencing data

2.3.1.1 Quality Control and Trimming

The raw fastq sequences were assessed using FastQC (0.11.8) (Andrew, S., 2010), available at http://www.bioinformatics.babraham.ac.uk/projects/fastqc/. The resulting FastQC files were summarized in MultiQC (Ewels et al., 2016), a time saving solution when having a large number of samples. The sequences were trimmed using Trim Galore (0.6.2), which is a wrapper of the Cutadapt program from Martin M. (2011), and available at: http://www.bioinformatics.babraham.ac.uk/projects/trim_galore/. The quality threshold was set to 30. A new FastQC and MultiQC report was conducted to confirm that both adapters, remaining from the sequencing process, and low-quality areas were removed from the sequences after trimming.

2.3.1.2 Reference genome

The reference genome used in this study was assembled by David Peris Navarro, as described in (Peris et al., *in prep*), using PacBio and Illumina reads of a North American specimen of *T. abietinum* collected in New Brunswick, Canada.

2.3.1.3 Mapping

The trimmed reads were mapped to the reference genome using the Burrows- Wheeler Alignment tool (BWA – 0.7.1) (Li & Durbin, 2010). This is a read alignment package that is based on backward searches using the Burrow-Wheeler Transform (Li & Durbin, 2010). It conducts alignments of short, low divergent sequencing reads against a large reference genome, like what is used for this analysis, and allows both mismatches and gaps (Li & Durbin, 2010). The SAM- file format, the output of the BWA, was converted to its binary equivalent BAM, using SAMtools (1.9) (Li et al., 2009), which takes up less space. The files were also sorted and indexed using SAMtools (1.9). Duplicate reads in the mapping were marked using GATK Mark Duplicates (4.1.4.0) (Van der Auwera & O'Connor, 2020), and then indexed again with SAMtools (1.9).

2.3.1.4 SNP Calling and Filtering

SNP calling was performed using GATK Haplotype Caller (Poplin et al., 2018), in GATK (4.1.4.0), which gives an output of one GVCF- file per sample. GenomicsDBImport (GATK 4.1.4.0) was used to make a database for these GVCF- files, which was used to combine the files for each sample into a single GVCF file using the GATK (4.1.4.0) joint genotyping.

BCF-tools (1.9) was used both for extracting quality measurements from the GVCF-file and for the quality filtering of it. Thresholds were set, in line with GATKs recommendations, as follows: The Fisher Strand value (FS), a Phred scaled probability for strand bias at a given site, was set to FST > 40. Strands Odds Ratio (SOR), another measurement for a strand bias, was set to SOR > 3. RMS Mapping Quality (MQ), measure for mapping quality was set to MQ > 40. Mapping Quality Rank Sum Test (MQRankSum) compares mapping qualities of reads supporting the reference and was set to MQRankSum > -5 and MQRankSum < 5.0. Quality by depth (QD) is the confidence in call, normalized by read depth at a site and was set to QD > 2. Read Position Rank Sum Test (ReadPosRankSum) measures relative positions of the reference versus the alternative allele in reads and was set to ReadPosRankSum >-4.0. Combined depth across samples (INFO/DP) is the sum of the read depth over all samples and was set to INFO/DP > 2x Mean DP

The SNP data remaining from the previous steps were further filtered with BCFtools (1.9) as follows: Single genotypes with low confidence scores, GQ < 20, were filtered out and a minimum read depth was set to DP < 3. Monomorphic SNPS (that was called because it differs from reference, but is not polymorphic in sample) was removed. And then a second filtering retaining only biallelic SNPs was performed. SNPs situated closer than 10 bp to indels were also filtered out because these are likely to be misaligned. Samples that were missing more than 70% of the data was removed, as well as sites where more than 20% of the samples were missing a genotype. Lastly, the data was filtered on Minor Allele Frequency (MAF). Variants with very low MAF-values may result from erroneous calls rather than representing real SNPs. The MAF value was set to be 0.05 in this case, which means that at a minimum of 5% of samples must have the same variant of a SNP to be included. SNP calling and filtering resulted in a dataset of 1,163,262 SNPs, used for further analyses.

2.3.2 Investigating population structure

2.3.2.1 Principal Component Analysis

A Principal Component Analysis (PCA) was performed to investigate the population structure based on allele frequencies of all samples. The analysis was conducted using Eigensoft (7.2.1) (Patterson et al., 2006). This package combines population genetics methods from Patterson et al., 2006 and stratification correction method from Price et al., 2006. Eigensoft requires files to be in a ped format, so vcf-files were first converted to ped using PLINK (1.9). A Principal Component analysis is a multivariate technique used to display observations as positions in an ordination space constructed from continuous axes summarizing the variation from all the variables (Duforet-Frebourg et al., 2016; Poplin et al., 2018). In this case the analysis outputs each sampled individual's coordinates along the principal component axes of variation (Alexander & Lange, 2011), to summarize differences and similarities between individuals based on allele frequencies. A disadvantage of the method is that PCA in some cases capture linkage disequilibrium instead of actual population structure (Privé et al., 2020). In this study this has been accounted for by pruning linked variants, to be able to quantify the most unbiased genetic structure in the data, as suggested in Gibson & Moyle (2020). Additionally, two samples with a high percentage of missing data (70%), and markers where more than 20% of the samples lack genotype information, were removed to eliminate the problem of detecting sample outliers as described in Gibson & Moyle (2020). The visual representation of the results from the analysis was made using ggplot2 (Wickham, 2011) in R (1.4.1106).

2.3.2.2 Admixture

Admixture (1.3.0)(Alexander & Lange, 2011) was used to estimate individual ancestry for all samples based on the SNP data. Admixture computes maximum likelihood to identify clusters given K ancestral populations as predefined by the user, as described in Alexander & Lange (2011). In an admixed population, expected allele frequency of each individual is a linear mix of the frequencies of the parent populations (Patterson et al., 2006) and thus explains the proportion of genomic ancestry for each individual relative to the other samples. Before running the analysis, ped-files were converted to bed files using PLINK (1.9). Admixture (1.3.0) was run on Ks ranging from 1-6, and a Cross-Validation error test performed to indicate best grouping of the samples in parent populations based on allele frequencies of sample input and range of Ks (Alexander & Lange, 2011). The visual representation of these results was constructed using the "barplot" function in R (version 1.4.1106).

2.3.2.3 Sliding Window Genome Scan

A Sliding Window Genome Scan analysis was performed to detect regions of divergence using a script developed by Simon Martin, available at https://speciationgenomics.github.io/sliding_windows/. The analysis was performed with a window size of 20 kb, sliding by 10 kb and with a minimum number of 10 kb sites covered. The analysis computes the Fixation index (Fst), Absolute divergence (Dxy), and nucleotide diversity (pi) for each population in genomic windows along the genome. Dxy and pi require monomorphic sites to be present in the dataset used, so a new filtering was performed keeping these sites, while other filtering settings remained as previously set, except an exclusion of MAF-filtering. Visual representations have been constructed using the "plot" function in R (1.4.1106).

2.3.3 Investigating genomic correlation to climatic variables

2.3.3.1 Redundancy Analysis

A Redundancy Analysis (RDA) was performed, correlating the SNP dataset to environmental variables (predictors), to investigate possible adaptation to local climates in the different groups of *T. abietinum*. The Analysis was performed in R (1.4.1106), using a script modified by Jørn Henrik Sønstebø together with a script authored by Brenna R. Forester available at https://popgen.nescent.org/2018-03-27_RDA_GEA.html, based on Forester et al. (2018). The script was run using the following packages: vcfR (Knaus & Grünwald, 2017), vegan (Oksanen et al., 2009), stringr (Wickham, 2019) and the R package parallel. RDA is a multivariate ordination technique able to analyse a large number of loci and environmental variables simultaneously to detect loci under selection for specific variables (Capblancq et al., 2018; Forester et al., 2018). RDA expose how groups of loci arrange themselves in a multivariate ordination space created by axes consisting of combinations of known variables (Rellstab et al., 2015; Forester et al., 2018). The analysis works in two steps: Multivariate linear regression is applied on genetic and environmental data, producing a matrix consisting of fitted values (Legendre & Legendre, 2012). The second step is a PCA of the fitted values producing canonical axes, these are linear combinations of the predictor variables (Legendre & Legendre, 2012). Because the complete vcf-file is very large, a random subsampling was taken from the original SNP dataset. GATK (4.1.4.0) was used to make a new, randomly sampled dataset containing 10% of the of the original genomic data, resulting in a sub sampled dataset of 115808 SNPs.

Both the RDA model and the axes were tested for significance using the "anova.cca" function in the vegan package (Oksanen et al., 2009) in R (1.4.1106), which is an ANOVA like permutation test. The "cca" function performs a correspondence analysis providing a robust test of the significance when there is a small dataset and the assumption of multinormality is not met (Legendre & Legendre, 2012). Because RDA is a linear model it assumes linear dependence between response variables and the explanatory variables (Legendre & Legendre, 2012). When testing the model in this study, the null hypothesis was that there is no linear relationship between the SNP data and the four environmental variables used. The alternative hypothesis was that there is a linear relationship between the SNP data and the environmental data. A calculation of R^2, the coefficient of determination, a statistical measure of how close the data are fitted to the regression line, was performed. 100% indicates that the model explains all the variability of the response data around its mean. Using Eigenvalues, the importance of each component to the total variability explained by the model was calculated.

Candidate SNPs, possibly under selection, was identified from SNPs connected to the different axes, calculated by RDA. Only SNPs from the RDA1 axis, already calculated as significant from the permutation test, was extracted with a 3 standard deviation cut-off (two-tailed p-value = 0.0027). Genomic locations of significant SNPs were investigated in an annotated genome of *T. abietinum.*

The predictor variables used in the RDA are geographically specific climate variables obtained from a previous dataset specific for Norway (Horvath et al., 2019) The following climatic variables were used in the analysis: Bioclim_1: Annual Mean temperature, Bioclim_12: Annual Precipitation, Bioclim_3: Isothermality and Bioclim_8: Mean Temperature of Wettest Quarter. An important factor classifying the different areas of sampling, and a main focus in this study is the differences between a coastal or a continental climate. The representative zones range on a main scale from wet to dry conditions and high and low isothermality. An isothermal value of 100 indicates a diurnal temperature range equivalent to annual temperature range (O'Donnell & Ignizio, 2012). With low values of isothermality there are smaller levels of temperature variability within an average month than what it is relative to a year (O'Donnell & Ignizio, 2012). There is a great difference in how the seasons change in relation to temperature, with more extremes in continental areas in contrast to a relatively stable coastal climate (Harstveit, 2015). For these reasons the variables of Annual Mean Temperature, Annual precipitation, Isothermality and Mean Temperature of Wettest Quarter has been chosen for the analysis.

Based on the sampling sites, these variables are hypothesized to have a great impact on the differences and potential adaptation in the populations of *T. abietinum.*

Because RDA is based on regression methods, a high correlation between the different climate variables used in the analysis could have an impact on the results (Dormann et al, 2013). Following the recommendations from Dormann et al. (2013), no variables used in the RDA correlates more than 0.56561. The different candidate variables were tested using the "cor.test" function in R (1.4.1106). This function is a test for association between paired samples, in this case using Kendall's Tau method (Hollander & Wolfe, 1973). The test is non-parametric and estimates a rank- based measure of association between the variables, and can be used if there is not a bivariate normal distribution (Hollander & Wolfe, 1973). Following the recommendations from Dormann et al (2013), no variables used in the RDA correlates more than 0.56561. Visual representations of the results from the Redundancy Analysis have been constructed in R (1.4.1106) using the plot function.

2.4 Common Garden experiments

2.4.1 Growth

Growth experiments were used to test for phenotypic differences between groups. Since *T. abietinum* is predominantly growing as dikaryons in nature, I established dikaryotic cultures by crossing selected monokaryons from the same populations. All cultures were investigated for clamps to confirm successful mating and a dikaryotic stage. Hyphal extension rate of the dikaryotic cultures were tested on: 12 ℃, 22 ℃ and 32 ℃. These temperatures were chosen based on previous literature on growth experiments for wood decay basidiomycetes (Maynard et al., 2019), as well as the conditions at the sampling site (Table 1). My goal was to cover most of the growth response curve, including the upper and lower temperature limits. Each culture was replicated three times on each treatment, to evaluate experimental biases and the isolates variability in growth. Small pieces of dikaryotic mycelium of the same size, stamped out with the back end of a 1250 µL pipette tip, were transferred to new MEA plates. Plates were then placed in three dark incubator cabinets, each with three different temperatures (12 ℃, 22 ℃ and 32 ℃. The temperatures of the cabinets were confirmed with a built-in thermometer in the cabinet, and a second thermometer as a control. After ten days, radial growth of each culture was measured using a digital calliper. The length of the experiment was set to ensure

measurable growth for slow growing cultures, and for fast-growing cultures to not be hindered by the limits of the petri dishes.

2.4.2 Decay

The same dikaryons were used in a wood decay experiment to observe potential differences in decay between groups. Each dikaryon was replicated three times, as in the growth experiment. The experiment was set up on wood blocks of *Picea abies*. Before the experiment, wood blocks were dried for 48 hours and immediately weighed. To make the wood blocks sterile, they were autoclaved three times each (with 24 hours between each session), and then soaked in autoclaved water straight after for 24 hours. On the day of the setup, wood-blocks were dipped in an autoclaved nutrient solution: 30 g/L $C_{12}H_{22}O_{11}$, 1 g/L $C_5H_{10}NNaO_5$, 1 g/L KH_2PO_4, 0.5 g/L $MgSO_4*7H_2O$, 0.01 g/L $FeSO_4*7H_2O$ (Capex Dox ÷ agar), and distilled water, to stimulate inoculation of the wood blocks. Wood blocks were put on a square nylon sheet in petri dishes containing Capex Dox ÷ Sucrose. A piece of each dikaryotic culture of the same size (stamped out using the backend of a 1250 µL pipette tip), were placed on the wood-block and left in a dark incubator at 22 °C. After 60 days the blocks were carefully scraped for mycelia, dried for 48 hours and reweighed to calculate the percentage of mass loss.

2.4.3 Statistical testing of experiments

To test the results from the common garden experiments for statistical significance, supporting the observed differences of hyphal extensive growth and wood mass loss between the groups, both datasets were tested with a Kruskal Wallis-test. The Kruskal-Wallis test is adapted to work for smaller dataset (Khan & Rayner, 2003; Tomczak & Tomczak, 2014). In this test, neither normality of residuals or response variables, nor heterogeneity of variance between predefined groups, are an assumption, as it is in a classical ANOVA and it is therefore better suited for these data (Khan & Rayner, 2003; Tomczak & Tomczak, 2014).

To test correlation between hyphal extension rate and decay the "cor.test" function in R (1.4.1106) was used, with non-parametric Kendall's Tau method (Hollander & Wolfe, 1973).

Table 1: All samples of *Trichaptum abietinum* collected and included in the present study. The columns describe: Location, Sample ID (the unique number of each monokaryon), Dikaryon ID (the ID for the dikaryon used in the experiments, each ID applies for the two monokaryons that were mated, bold refers to selfed dikaryons mating with spores from same fruit body), number of Mapped reads to the reference genome, Mapping percentage, Location Coordinates, Annual Mean Temperature (Bioclim 1) in °C, Isothermality (Bioclim 3), Mean Temperature of Wettest Quarter (Bioclim 8) in °C and Annual Precipitation (Bioclim 12) in mm.

Location	Sample ID	Dikaryon ID	Mapped reads	Mapping %	Location Coordinates	Bioclim 1 (AMT)	Bioclim 3 (Iso)	Bioclim 8 (MTWQ)	Bioclim 12 (AP)
Puttåsen	TA-1024-2-M1	D22	5129893	83.31	59°54'52''N, 10°54'0''E	4.054696083	44.19031906	14.87906647	991.4177246
Puttåsen	TA-1024-4-M1	D24	3347471	80.26	59°54'52''N, 10°54'0''E	4.054696083	44.19031906	14.87906647	991.4177246
Puttåsen	TA-1024-5-M3	D24	8701861	81.23	59°54'52''N, 10°54'0''E	4.054696083	44.19031906	14.87906647	991.4177246
Puttåsen	TA-1024-7-M1	D21	4419731	83.06	59°54'52''N, 10°54'0''E	4.054696083	44.19031906	14.87906647	991.4177246
Puttåsen	TA-1024-8-M1	D22	5346870	83.46	59°54'52''N, 10°54'0''E	4.054696083	44.19031906	14.87906647	991.4177246
Puttåsen	TA-1024-9-M3	D23	4355667	75.66	59°54'52''N, 10°54'0''E	4.054696083	44.19031906	14.87906647	991.4177246
Puttåsen	TA-1124-8-M2	D21	x	x	59°54'52''N, 10°54'0''E	4.054696083	44.19031906	14.87906647	991.4177246
Puttåsen	TA-1124-3-M2	D23	x	x	59°54'52''N, 10°54'0''E	4.054696083	44.19031906	14.87906647	991.4177246
Lalm	TA-1089-M3	D1	12360195	86.64	61°47'57''N, 9°18'58''E	1.381604195	44.56803131	13.05561638	496.7272034
Lalm	TA-1090-M1	D1	10415688	88.58	61°47'57''N, 9°18'58''E	1.381604195	44.56803131	13.05561638	496.7272034
Lalm	TA-1092-M1	D2	5380111	81.00	61°47'57''N, 9°18'58''E	1.381604195	44.56803131	13.05561638	496.7272034
Lalm	TA-1093-M1	x	6199527	84.90	61°47'57''N, 9°18'58''E	1.381604195	44.56803131	13.05561638	496.7272034
Lalm	TA-1094-M1	D2	5131649	82.30	61°47'57''N, 9°18'58''E	1.381604195	44.56803131	13.05561638	496.7272034
Lalm	TA-1096-M1	x	6364764	77.76	61°47'57''N, 9°18'58''E	1.381604195	44.56803131	13.05561638	496.7272034
Lalm	TA-1099-M1	x	6263537	84.27	61°47'57''N, 9°18'58''E	1.381604195	44.56803131	13.05561638	496.7272034
Lalm	TA-1100-M2	**D3**	x	x	61°47'57''N, 9°18'58''E	1.381604195	44.56803131	13.05561638	496.7272034
Lalm	TA-1098-M1	**D4**	x	x	61°47'57''N, 9°18'58''E	1.381604195	44.56803131	13.05561638	496.7272034
Atna	TA-1103-M2	D7	7665580	72.16	61°38'54''N, 10°52'56''E	1.001416683	42.82033157	13.52506638	558.3670044
Atna	TA-1104-M2	D8	10403117	86.21	61°38'54''N, 10°52'56''E	1.001416683	42.82033157	13.52506638	558.3670044
Atna	TA-1105-M3	D5	6377943	86.90	61°38'54''N, 10°52'56''E	1.001416683	42.82033157	13.52506638	558.3670044
Atna	TA-1106-M2	D6	5035059	88.44	61°38'54''N, 10°52'56''E	1.001416683	42.82033157	13.52506638	558.3670044
Atna	TA-1107-M2	D5	6052686	87.69	61°38'54''N, 10°52'56''E	1.001416683	42.82033157	13.52506638	558.3670044
Atna	TA-1108-M1	D7	6849634	78.45	61°38'54''N, 10°52'56''E	1.001416683	42.82033157	13.52506638	558.3670044
Atna	TA-1110-M1	D6	10272834	85.23	61°38'54''N, 10°52'56''E	1.001416683	42.82033157	13.52506638	558.3670044
Atna	TA-1111-M1	D8	4328104	89.74	61°38'54''N, 10°52'56''E	1.001416683	42.82033157	13.52506638	558.3670044
Modalen	TA-1126-M1	D10	8045622	85.84	60°49'15''N, 5°45'42''E	4.379929066	47.24007416	0.568383455	3636.619385
Modalen	TA-1127-M1	D9	7870779	89.03	60°49'15''N, 5°45'42''E	4.379929066	47.24007416	0.568383455	3636.619385
Modalen	TA-1129-M1	D11	11673773	87.87	60°49'15''N, 5°45'42''E	4.379929066	47.24007416	0.568383455	3636.619385
Modalen	TA-1130-M1	D12	6993464	87.17	60°49'15''N, 5°45'42''E	4.379929066	47.24007416	0.568383455	3636.619385
Modalen	TA-1133-M3	D11	6279490	85.57	60°49'15''N, 5°45'42''E	4.379929066	47.24007416	0.568383455	3636.619385
Modalen	TA-1134-M1	D10	6871547	70.57	60°49'15''N, 5°45'42''E	4.379929066	47.24007416	0.568383455	3636.619385
Modalen	TA-1136-M1	D12	8616042	89.43	60°49'15''N, 5°45'42''E	4.379929066	47.24007416	0.568383455	3636.619385
Modalen	TA-1137-M1	D9	6821344	85.89	60°49'15''N, 5°45'42''E	4.379929066	47.24007416	0.568383455	3636.619385
Arendal	TA-1139-M1	D15	6175940	85.00	58°29'41''N, 8°41'44''E	7.103533268	44.45862961	3.021633387	1312.775391
Arendal	TA-1140-M1	x	8163916	90.30	58°29'41''N, 8°41'44''E	7.103533268	44.45862961	3.021633387	1312.775391
Arendal	TA-1141-M2	D14	7391453	87.98	58°29'41''N, 8°41'44''E	7.103533268	44.45862961	3.021633387	1312.775391
Arendal	TA-1142-M1	D15	4816060	83.50	58°29'41''N, 8°41'44''E	7.103533268	44.45862961	3.021633387	1312.775391
Arendal	TA-1146-M2	D14	9342945	87.31	58°29'41''N, 8°41'44''E	7.103533268	44.45862961	3.021633387	1312.775391
Arendal	TA-1149-M1	**D13**	x	x	58°29'41''N, 8°41'44''E	7.103533268	44.45862961	3.021633387	1312.775391
Arendal	TA-1145-M1	**D16**	x	x	58°29'41''N, 8°41'44''E	7.103533268	44.45862961	3.021633387	1312.775391
Bø	TA-1150-M3	**D18**	x	x	59°24'52''N, 8°58'23''E	5.593770981	43.71965027	14.76335049	1135.657227
Bø	TA-1151-M1	D17	7881749	89.30	59°24'52''N, 8°58'23''E	5.593770981	43.71965027	14.76335049	1135.657227
Bø	TA-1152-M1	D19	8579954	86.67	59°24'52''N, 8°58'23''E	5.593770981	43.71965027	14.76335049	1135.657227
Bø	TA-1153-M2	D17	6417301	87.95	59°24'52''N, 8°58'23''E	5.593770981	43.71965027	14.76335049	1135.657227
Bø	TA-1154-M2	x	6773329	91.13	59°24'52''N, 8°58'23''E	5.593770981	43.71965027	14.76335049	1135.657227
Bø	TA-1159-M2	D20	x	x	59°24'52''N, 8°58'23''E	5.593770981	43.71965027	14.76335049	1135.657227
Bø	TA-1156-M1	D20	7582126	89.31	59°24'52''N, 8°58'23''E	5.593770981	43.71965027	14.76335049	1135.657227
Bø	TA-1158-M2	D19	5514695	82.95	59°24'52''N, 8°58'23''E	5.593770981	43.71965027	14.76335049	1135.657227

3 Results

3.1 Population structure

I first tested whether any genetic structure could be found across the sampled populations. In the Principal Component Analysis (PCA), five of the populations (Arendal, Atna, Lalm, Puttåsen and Bø) showed high similarity in allele frequencies, and no clear genetic structure (Fig. 2). On the contrary, the population from Modalen separated from the other populations along PC1, explaining 4.81% of the variance, and showed clear differences in allele frequency compared to the other group (Fig. 2).

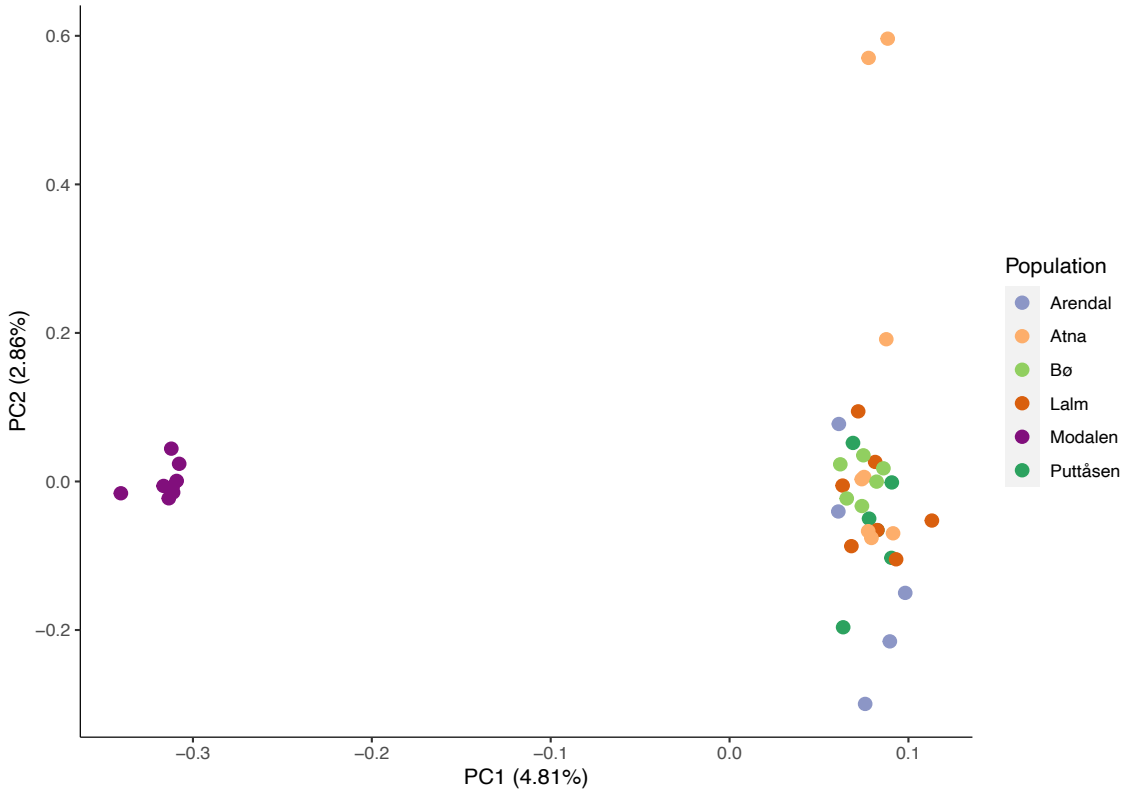

Figure 2: Principal Component Analysis, describing the population structure of sampled specimens of *Trichaptum abietinum,* based on a linkage-pruned SNP dataset of 56,070 SNPs of 40 monokaryotic specimens. Each dot represents an individual and the color describes the associated population, and thus sampling site. The axes describe 4.81% (PC1) and 2.86% (PC2) of the variation observed in the data.

In line with the PCA, the Admixture analysis divided the samples into two groups of diverging ancestry, separating Modalen from the main group of populations (Fig. 3a). Hence, K = 2 had the lowest CV error (1.38) compared to other K values (Fig. 3b). Two individuals from Arendal in the main group, showed slight admixture with the Modalen group (Fig. 3a).

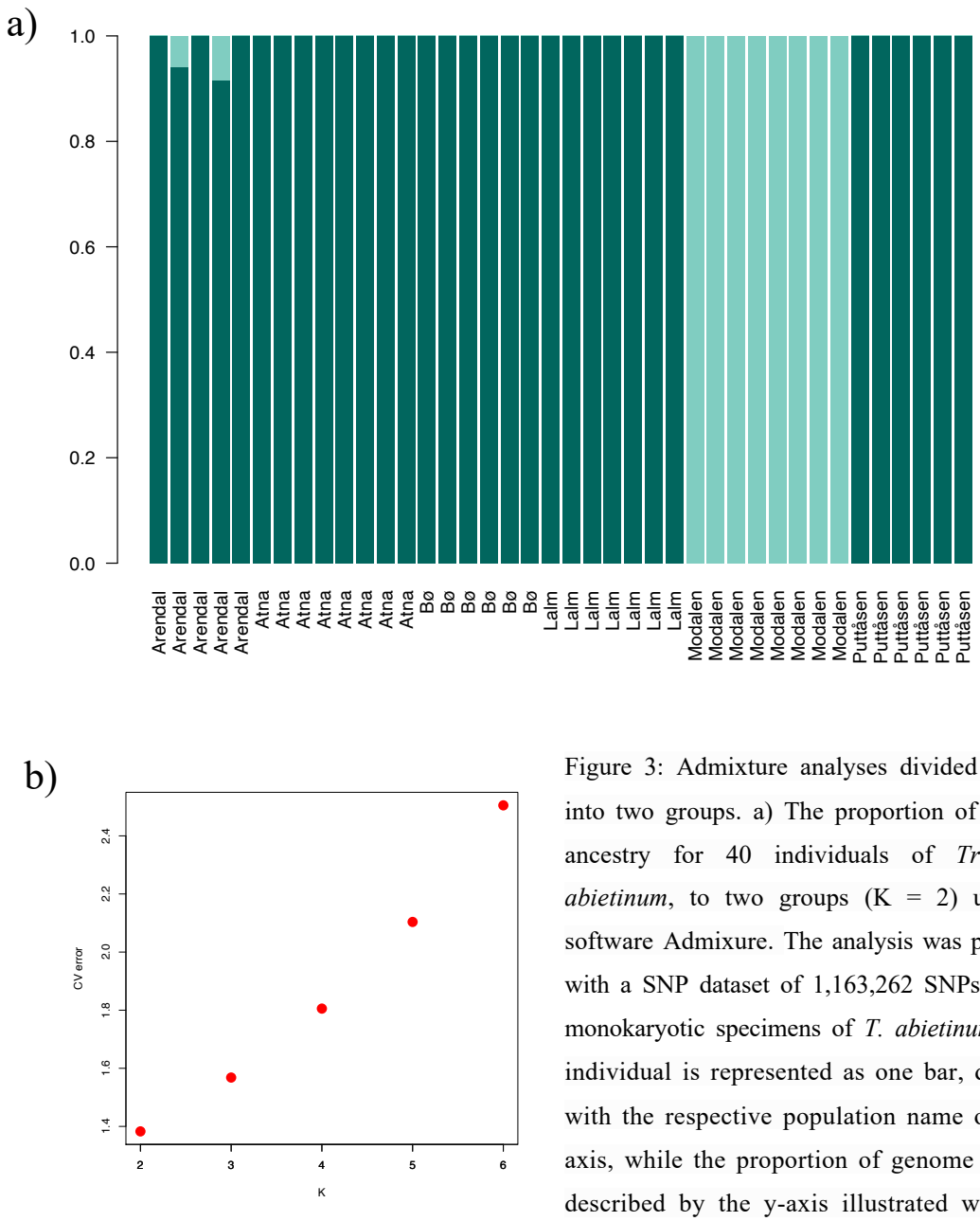

Figure 3: Admixture analyses divided the data into two groups. a) The proportion of genomic ancestry for 40 individuals of *Trichaptum abietinum*, to two groups (K = 2) using the software Admixure. The analysis was performed with a SNP dataset of 1,163,262 SNPs from 40 monokaryotic specimens of *T. abietinum*. Each individual is represented as one bar, described with the respective population name on the x-axis, while the proportion of genome origin is described by the y-axis illustrated with color codes describing the two ancestral groups. b) K = 2 is presented as this had the lowest Cross Validation error for Ks ranging from 1-6.

The results from the Genome Scan supports the pattern observed in the PCA and Admixture Analysis. The Fixation index (Fst) mean value are just above zero, and the absolute divergence (Dxy) mean value between 2.7 and 2.8 for populations from Bø and Lalm (Fig. 4a-c). Similar results were observed for all other populations in the main group. Figure 4a-c illustrates a selected example of the observed pattern consistent for all populations within the main group. The observed divergence between Modalen and populations from the main group was higher, with Fst mean values around 0.15 (Fig. 4d). All scaffolds show long tails of divergent genomic regions with high Fst values, several of them reaching above 0.8 on the y axis. The absolute divergence (Dxy) showed mean values around 0.37. Figure 4d illustrates a selected example of the observed pattens of divergence between Modalen and populations from the main group. The samples from Modalen also holds a higher genetic variability within the population gene pool, with a mean pi value of 0.33, compared to mean pi values between 0.27 and 0.28 for the remaining populations (Fig. S1).

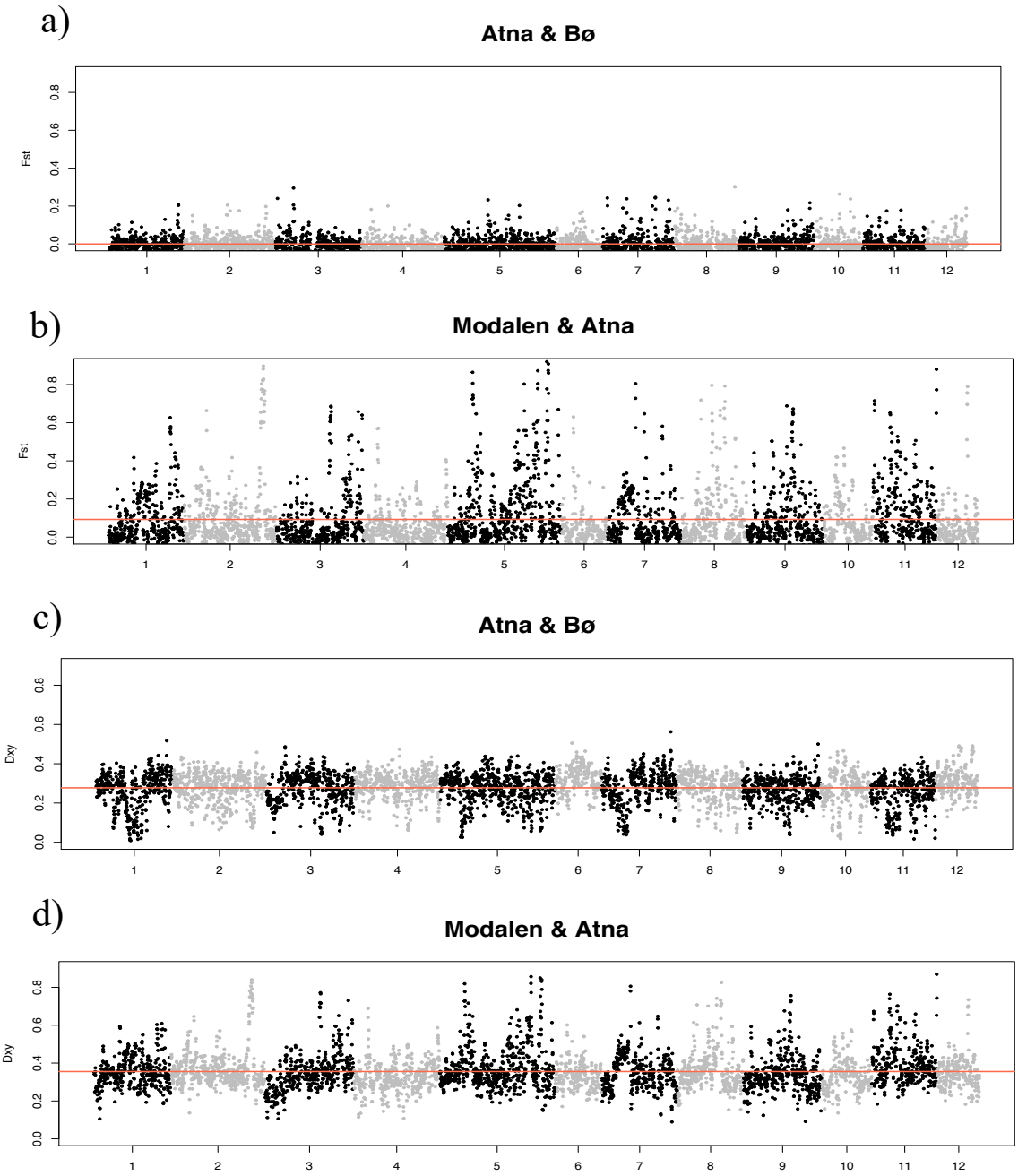

Figure 4: Scatter plots from sliding window genome scans of Fixation index (Fst) and absolute divergence (Dxy) along the genomes of two selected populations of *Trichaptum abietinum*, using a SNP dataset of 1,163,262 SNPs. Each plot represents Fst or Dxy value for one sliding window (20 kb) from the genome scan. Scaffolds, from 1-12, are illustrated along the x-axis, while the y-axis represents the Fst or Dxy values, ranging from 0-1. The horizontal line (red) marks the mean value. (a) Show the Fst-values of the different sliding windows along the genomes of populations from Atna and Bø. (b) Show the Fst-values of the different sliding windows along the genomes of populations from Modalen and Atna. (c) Show the Dxy-values of the sliding windows along the genomes of populations from Atna and Bø. (d) Show the Dxy values of the sliding windows along the genomes of populations from Modalen and Atna.

3.2 Adaptation to climatic variables

In the Redundancy Analysis I investigated if local adaptation within populations could be identified, by correlating the genetic variation to four climatic variables. A calculation of the adjusted coefficient of determination showed a value of 0.0796, which means the model explained 7.96% of all the variability of the response data around its mean (p-value < 0.001). Analysis of eigenvalues showed that RDA1 explained 61.9% of the total variability captured by the model, RDA2 explained 13.0%, RDA3 12.7% and RD4 12.2%. However, only RDA1 was significant (p-value < 0.001). All four climate variables used in the analysis: Annual Mean Temperature, Annual Precipitation, Isothermality and Mean Temperature of Wettest Quarter, was tested against each other, with less than a correlation of 0.54 with any other variable. The ordination created from RDA indicated that the significant RDA1 correlated with the predictor variables Mean Annual Precipitation and Isothermality. All eight samples from Modalen were positively correlated to both these bioclimatic variables along the RDA1 axis (Fig. 5). The RDA2 axis suggest to partly correlate to the bioclimatic variable Annual Mean Temperature. All samples from Arendal were positively correlated to Annual Mean Temperature (Fig. 5), but the RDA2 axis was not found to be significant (p = 0.996).

RDA identified 2091 SNPs correlating to the different predictor variables. In total 275 SNPS correlated with Isothermality, 315 with Temperature of Wettest Quarter, 1164 with Annual Mean Temperature and 337 with Annual Precipitation. Of all these SNPs, 266 were found to be significant candidate loci, with a 3 standard deviation cut off (a two tailed p value = 0.0027). All these were connected to the RDA1 axis. Out of the 266 significant SNPs, 263 showed the highest correlation to the predictor variable Annual Precipitation, and 3 to Isothermality (Table S1). Most of these SNPs were found in annotated genes (Table S1), but their functions need to be further investigated (Peris et al., *in prep*.). In total, 106 genes of known and unknown functions were identified in these locations (Table S1).

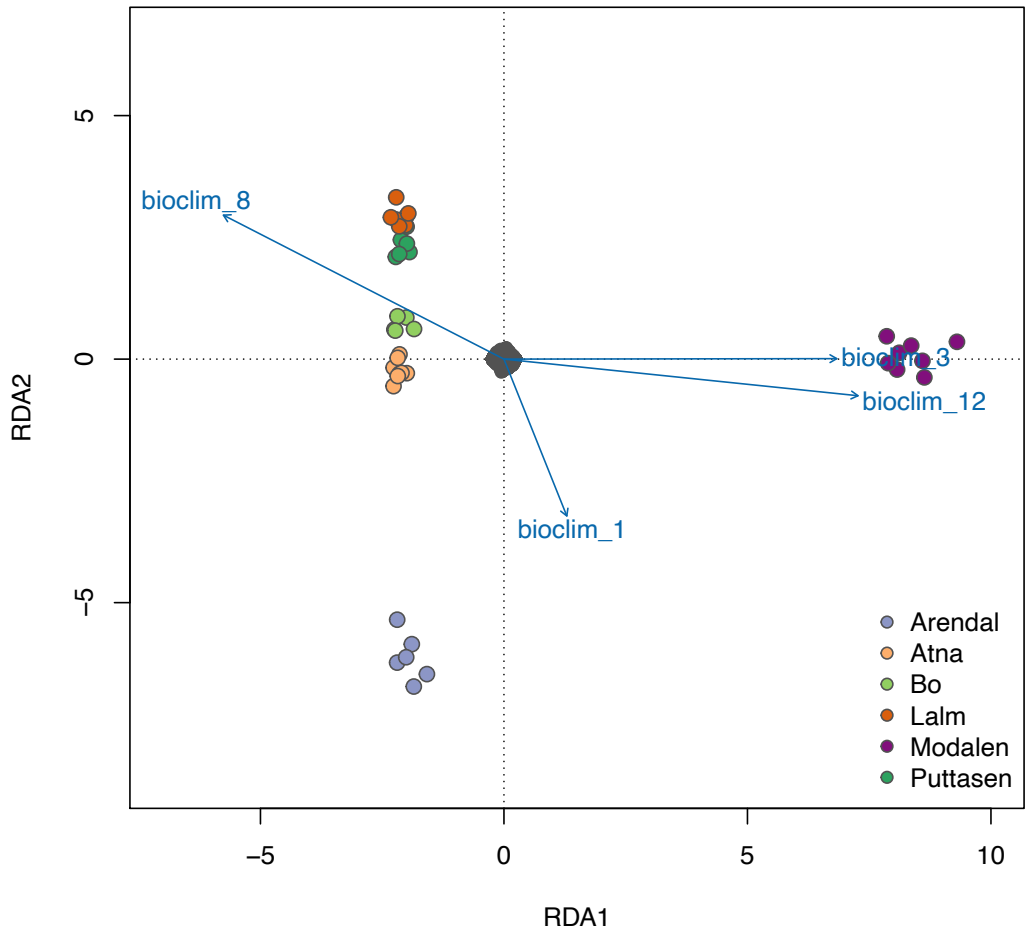

Figure 5: A multivariate ordination plot describing the relationship between SNPs from sampled specimens of *Trichaptum abietinum* and four climatic variables. The analysis was performed with a random sub sampled SNP dataset of 1,163,262 SNPs from 40 monokaryotic specimens. The colored dots represent samples, colored after population. Individuals are arranged in an ordination space to describe the relationship between the genomic samples along the RDA1 and RDA2 axes summarizing the variation of the predictor variables. RDA1 axis explains 61,9 % and RD2 13,0% of the variation explained by the model (7,96% of total variation). The predictor variables correlated with the axes are depicted as vectors (In blue). Bioclim_1 is Annual Mean Precipitation, Bioclim_3 is Isothermality, bioclim_8 is Mean Temperature of Wettest Quarter and bioclim_12 is Annual Precipitation. The SNPs are illustrated in the center of the plot, marked in dark grey.

3.3 Phenotypic differences

In the growth experiments, I wanted to test whether there were differences in hyphal extension rate on different temperatures, or differences in decay between the various populations (Fig. 6-8). Results from a Kruskal Wallis test showed that there were no significant differences in growth between the populations in any of the three temperatures, with a p = 0.45 n 12 °C, p = 0.34 on 22 °C and 0.22 on 32 °C. Neither in the decay experiment, significant differences were detected between groups in relation to percentage of mass loss. However, clear trends were observed with a consistent pattern of differences between groups on all temperatures. Specimens from Modalen showed the fastest hyphal extension rate on all three temperatures, while specimens from Arendal had one of the lowest, together with specimens from Atna and Lalm (Fig. 6-7). All populations, some to a higher degree than others, showed a decline in hyphal extension rate at 32 °C (Fig. 6-7). The result from the decay experiment, seem to mirror the result from the hyphal extension rate experiments to a large extent, with much of the same patterns observed between groups (Fig. 8). Individuals with fast hyphal extension rate also have a high percentage of wood mass loss, but no significant correlation between growth and decay was detected when tested. Replicates with less than 5% mass loss was removed from the wood-decay dataset due to unsuccessful inoculation of the wood blocks. This was done to avoid unrepresentative decay rates for some individuals. The removal of these replicates resulted in uneven group sizes in the decay experiment.

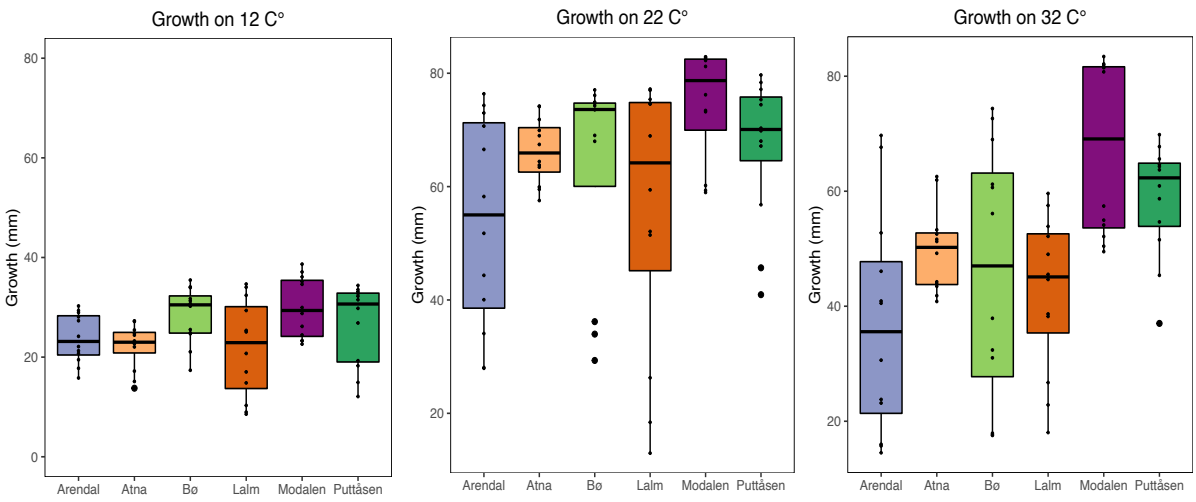

Figure 6: Boxplot illustrating the hyphal extension rate of dikaryotic individuals of *Trichaptum abietinum* on three different temperatures 12, 22 and 32 °C. Dikaryons were crossed from haploid monokaryotic cultures from the same population, for each of six populations. Each group contains four dikaryons. The color of the boxes represents the respective population of the dikaryotic individuals. The y- axis describes the mean hyphal extension rate (in mm). The horizontal lines in each box represents the median and the upper and lower part of the boxes represents the 25th and 75th percentiles. Each replicate measurement is marked with a dot. The lines extending from the boxes describes minimum or maximum values. The dots not connected to the extending lines represents outliers.

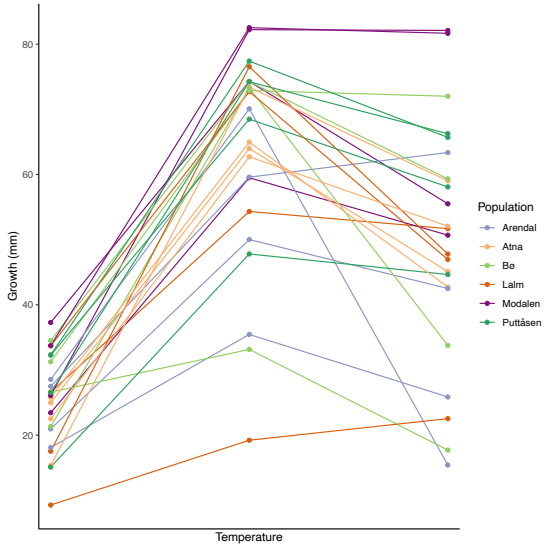

Figure 7: A lined scatterplot illustrating the growth progress of dikaryotic individuals of *Trichaptum abietinum* on three different temperatures: 12 °C, 22°C and 32 °C. The plots and lines are colored by the respective populations of the individuals. The growth, described by the y-axis, is measured in mm. The y-axis is discrete and describes the three different temperatures, 12, 22 and 32 °C.

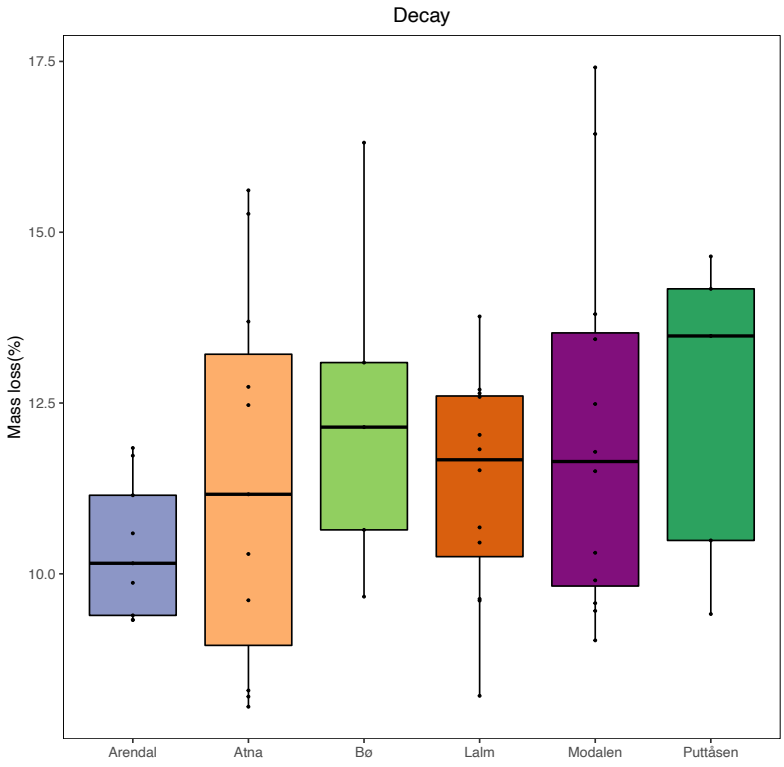

Figure 8: Boxplot illustrating the percentage of mass loss of wood being decayed by dikaryotic individuals of *Trichaptum abietinum* at 22 °C. Dikaryons were crossed from haploid cultures from six different sampled populations. Each group contains four dikaryons. The color of the boxes represents the respective population of dikaryotic individuals. The y- axis describes the decay in percentage of mass loss (measured in grams). The horizontal lines in each box represents the median and the upper and lower part of the boxes represents the 25th and 75th percentiles. Each replicate measurement is marked with a dot. The lines extending from the boxes describes minimum or maximum values.

4 Discussion

The widespread geographic distribution of *T. abietinum*, where it grows in a range of different habitats, suggests that there may be local adaptation or high plasticity in the different populations. I have investigated local adaptation in Norwegian populations of *T. abietinum* using population genomic analyses and common garden experiments. A clear genetic divergence between samples collected from the west coast and southeastern part of Norway was observed. This could indicate different immigration routes of the species into Norway after the last glaciation, and further complicates the question of local adaptation to diverging conditions between east and west. Genomic regions possibly connected to climatic variation, was revealed, including genes of both unknown and known gene functions.

The population structure among the sampled specimens demonstrated two clearly divergent genetic groups of *T. abietinum* in Norway, supported by PCA and Admixture Analysis, as well as the Fst values. Little divergence was found within these two different groups. Genetic diversity within populations was similar, with a slightly higher pi value observed in the Modalen population compared to the populations in the main group. Because of the substantial differences observed between the two groups, I suggest that the genetic divergence could be due to different immigration histories of the two groups of *T. abietinum*. In support of this, phylogenetic analyses of a larger sample of European collections of *T. abietinum* showed that all eight specimens sampled from Modalen groups together with central European populations of the species (Peris et al., *in prep*; Lu et al. *in prep.*). *Trichaptum abietinum* grows mostly on *Picea abies*, thus the history of *T. abietinum* could be tightly linked to the intricate, and much debated history of the Norwegian population of *P. abies*.

The leading theory behind the demographic history of *P. abies* has long been that the species immigrated from the east, via Finland and Sweden, and established in eastern parts of Norway around 1500-2000 years ago before it spread further north and westward (Huntley & Birks, 1983; Ohlson et al., 2011, Giesecke & Bennett, 2014) However, other studies, using both DNA and pollen fossil data, have indicated that *P. abies* survived *in situ* in local refugia on the west coast of Norway (Vorren & Mangerud 2006; Parducci et al., 2012). Further, analysis of cytoplasmic DNA markers, combined with palaeobotanical data, have identified two highly differentiated genetic groups of spruce, demonstrating that Siberian spruce and northern

European spruce are two different taxa, possibly caused by two separate LGM refugia (Tollefsrud et al., 2015). The possibility that *P. abies* immigrated from both the east and the west (or possibly survived *in situ*), raises the hypothesis that the genetic differences observed between the two groups of *T. abietinum* could be due to different demographic histories of the different populations of *P. abies* and *T. abietinum* in Scandinavia. Genetic divergence, caused by different post glacial immigration routes, have also been observed in two European oak species, *Quercus petrea* and *Q. pubescens* (Petit et al., 2002).

The source of the *P. abies* forest in Modalen has been debated, and it is uncertain whether it is planted by humans or if it has spread naturally (Øyen, 2017). The same is true for other spruce forests with unknown history along the west coast (Andersen et al., 1983; Øyen, 2017), areas with an extensive history of seaborn trade. The genetic differences dividing east and west could be further maintained by the large mountain chains separating western and eastern parts of Southern Norway, hindering gene flow between the groups.

The homogeneity observed between the populations in the main group indicate a substantial amount of dispersal ability and gene flow between these locations. This was supported by a previous study of *T. abietinum*, investigating three genetic markers in 11 Fennoscandian populations, showing that sampled populations had low levels of genetic differentiation and presumably high amounts of gene flow (Kauserud and Schumacher, 2003).

The RDA analysis indicated that the genotypes from Modalen were associated with high annual precipitation and isothermality. Considering the climatic conditions from the sample site in Modalen, these results fit my expectations. Most fungi are able to tolerate substantial variation in pH and temperature (Schimel et al., 2007; Crowther et al., 2014), but are highly responsive to changes in water availability (Kardol et al., 2010). Several studies have demonstrated that moisture stress, caused by factors like disturbance, fire, drought or freezing, is a dominant abiotic factor affecting fungal combative abilities (Magan & Lacey, 1984; Crowther et al., 2014). These studies further support that moisture and climatic stability seem to impose a strong environmental pressure driving selection compared to other factors like temperature, which is also proposed in the results from RDA in this study.

The population genomics analyses revealed that 266 SNPs were significantly correlated to predictor variables. From these SNPs, 263 had highest correlation with Annual Precipitation

and 3 to Isothermality. The 266 SNPs were located in regions with genes of both known and unknown functions in fungi or other organisms. 106 genes of known and unknown functions were identified in the positions of these 266 SNPs. However, a specific pattern of particular functions that are overrepresented in these 266 SNPs is not analysed, and not readily observable. Strong genomic signatures of positive selection and genomic sites associated with specific climatic regimes were found across North America in the ectomycorrhizal fungus *Suillus brevipes* (Branco et al. 2017). The authors argue that some of the regions under positive selection could be connected to cold stress response, i.e. transmembrane transport and helicase activity. Moreover, genomic regions of extreme divergence were also found in two recently diverged populations of *Neurospora crassa* (Ellison et al., 2011). Further investigation of these diverging regions revealed that several genes in these locations were involved in responses to cold temperatures (Ellison et al., 2011). Growth experiments further suggested that one population had a higher fitness on low temperatures (10°C), which was connected to the difference of 9 °C in average yearly minimum temperature between the two locations (Ellison et al., 2011). Precipitation and isothermality, has also been identified as the main predictors driving variation in wild tomato plants, using a Redundancy Analysis (Gibson & Moyle 2020). Moreover, they found that the environment explained more of the genomic variation than factors like geography, across populations inhabiting a wide range of different habitats in Ecuador and Peru (Gibson & Moyle, 2020), which is also what is indicated by the Redundancy Analysis in this study. Closer investigation of the significant genes found in in this study, and their gene functions, is needed to further explore the possible connection to adaptation to wet and stable climates in *T. abietinum*.

Due to the substantial genetic divergence found between the two groups, and the possible independent immigration histories from different refugia, it could be questionable to analyse the population from Modalen together with the other five populations in a Redundancy Analysis. RDA has not yet been extensively tested in situations with a distinct population structure (Forester et al. 2018). Due to limited computing capacity, only 10% of the genetic data was included in the RDA. This imposes a risk that important SNPS and diversity was not detected. However, the used dataset was obtained by a random sub sampling across the entire genome, thus it should not be biased to any particular genomic region.

The results from the growth experiment showed consistent trends for all temperatures, i.e. those speciemens with fastest hyphal extension rate for one temperature, had the fastest hyphal

extension rate for all temperatures. Another observed trend is that the individuals of fast hyphal extension rate, also had high percentages of mass loss in the decay experiment. A positive correlation of hyphal extension rate and decay rates were also found in Lustenhouwer et al. (2020). However, neither significant differences in hyphal extension rate between populations, nor a significant correlation between hyphal extension rate and decay were found. This could possibly be due to the considerably small group sizes used in the experiment. The speciemens from the western population (Modalen) had the fastest hyphal extension rate on all three temperatures. Because local adaptation is thought to generate high phenotypic variation within species (Gibson & Moyle, 2020), these results suggest adaptation towards fast hyphal extension rate in the Modalen population. Recent studies have shown that fungal genotypes with fast, explorative growth and high competitiveness, have low stress tolerance, and are selected for in environments with favorable conditions, i.e., moist and climatic stable environments (Crowther et al., 2014; Maynard et al., 2019; Lustenhouwer et al., 2020). On the contrary, more stressful conditions are thought to select for denser hyphal growth and higher stress tolerance, i.e., environments with large fluctuations in temperature and precipitation (Crowther et al., 2014; Maynard et al., 2019; Lustenhouwer et al., 2020). This theory represents a trade-off between competitive dominance and stress tolerance in fungi (Maynard et al., 2019; Lustenhouwer et al., 2020). The trade-off between competitiveness and stress tolerance in fungal genotypes have not been tested in this study, but the observed trends from the common garden experiment could coinside with this theory, considering climatic conditions on the sampling sites of the groups with fast hyphal extension rate and high percentage of wood mass loss.

Even though the western population may be divergent, with a different demographic history than eastern populations, it cannot be dismissed that some of the differences observed between the groups could be due to adaptation to local conditions. Especially considering the rather extreme climatic conditions at the sampling site in Modalen with regards to precipitation. Previous studies have found potential adaptation in fungal genotypes in response to both precipitation levels, isothermality and other climatic conditions (Ellison et al., 2011; Crowther et al., 2014; Branco et al., 2017; Maynard et al., 2019).

When looking at the five eastern populations separately, the only observed pattern in the RDA was a positive correlation between specimens from Arendal and Annual Mean Temperature (but not significant), which fits the expectations considering the local climate at the sampling site. The southern locality of Arendal receives substantially less precipitation compared to

Modalen, combined with the highest Annual Mean Temperatures of all locations. Frequent periods of warm weather and sparse precipitation could select for stress tolerant genotypes, as suggested by Maynard et al. (2019), and thus explain why specimens from Arendal had the lowest hyphal extension rate and the lowest amount of wood mass loss of all populations, although not significant. Thus, this suggested adaptation in Arendal to high temperatures cannot be confirmed. Fungal growth rate was found to be the strongest single predictor of fungal wood decomposition in laboratories (Lustenhouwer et al., 2020), where extension rates explained about 19% of the variance in decomposition (Lustenhouwer et al., 2020). Due to the small group sizes used, and few replicates, the results from the experiments might have been affected by random coincidences, like differences in fitness of the dikaryons. Other important selection factors, that might influence the fungus growth and decay rate, and how these relate to climate have not been considered. For example, under certain climatic conditions, biotic interactions influencing mycelial growth, might be stronger or weaker.

The population structure found in this study, supported by the low divergence found in populations of *T. abietinum* in Fennoscandia (Kauserud & Schumacher, 2003,) proposes a pattern of a more or less continuous population in eastern and southern parts of Norway with high gene flow. High similarity in allele frequencies in the main group, despite large geographic and climatic differences, could reflect the recent arrival of the eastern populations with *P. abies,* around 1500-2000 ago (Huntley & Birks, 1983; Ohlson et al., 2011; Giesecke & Bennett, 2014). The relatively recent post-glacial immigration of *T. abietinum* in eastern parts of Norway, combined with frequent gene flow between locations, could counteract clear local adaptation in eastern populations (Fisher, 1930; Slatkin, 1987). The absence of clear adaptation to local conditions could also suggests a high amount of phenotypic plasticity, supported by fungal trait responses observed to be highly plastic (Crowther et al., 2014), or a selection for stress tolerant genotypes as observed in other fungal studies (Crowther et al., 2014; Maynard et al., 2019).

Populations that are capable of adapting to a larger range of climatic conditions, either because they are adapted to endure high stress environments or due to high plasticity will be able to survive and adapt in face of future climatic alterations. In Lennon et al. (2012), they describe drought tolerant fungi as generalists, given the capability of existing along a broad moisture gradient. On the other hand, drought intolerant fungi are considered to be specialists, only capable of growing and competing under narrow range of climatic conditions (Lennon et al., 2012), and thus more vulnerable to climatic changes in regards to precipitation.

5 Conclusion and further studies

I suggest that the observed divergence between east and west could be due to different immigration routes of *T. abietinum,* possibly connected to separate post glacial immigration routes of *Picea abies*. Additionally, I have found some weak support for adaptation to local conditions that are especially different between east and west. The results obtained from the RDA, coupled with experiments on growth and decay suggest that there might be adaptation to high precipitation levels and isothermality in Modalen, and that the possible adaptation could be connected to a trade-off between competitive and stress tolerant genotypes. However, due to the distinct population structure between east and west the results from the RDA could be misinterpreted as local adaptation, while it may be a result of long-term divergence and/or adaptation to conditions in central Europe. Several genes were found in the regions of SNPs identified by the RDA as potentially under selection, possibly connected to adaptation to wet and stable conditions. I did not observe statistically significant differences between groups in regards to hyphal extension rate and decay when tested, possibly due to small group sizes.

In future studies more sample sites and a higher number of individuals in each population should be included. More populations from the west coast should be sampled to further investigate genetic differences between eastern and western groups. Populations from central Europe should also be included to further explore the genetic relationship between western and central European populations. A more detailed investigation of genes in areas under selection or that are correlated to specific climatic variables in *T. abietinum* could be done, similar to what has been done in Ellison et al. (2011). Branco et al. (2015; 2017) and Gibson & Moyle (2020). Moreover, it would be interesting to add variation in moisture as a factor in the common garden experiments because of the substantial differences in precipitation between western and eastern localities and because fungal species showing rapid hyphal extension rate has also been observed to have a narrow niche in regards to moisture (Maynard et al., 2019).

References

Aitken, S. N., Yeaman, S., Holliday, J. A., Wang, T., & Curtis-McLane, S. (2008). Adaptation, migration or extirpation: Climate change outcomes for tree populations. *Evolutionary Applications*, *1*(1), 95–111. https://doi.org/10.1111/j.1752-4571.2007.00013.x

Alexander, D. H., & Lange, K. (2011). Enhancements to the ADMIXTURE algorithm for individual ancestry estimation. *BMC Bioinformatics*, *12*(1), 246. https://doi.org/10.1186/1471-2105-12-246

Allison, S. D., Romero-Olivares, A. L., Lu, L., Taylor, J. W., & Treseder, K. K. (2018). Temperature acclimation and adaptation of enzyme physiology in *Neurospora discreta*. *Fungal Ecology*, *35*, 78–86. https://doi.org/10.1016/j.funeco.2018.07.005

Altschul, S. F., Gish, W., Miller, W., Myers, E. W., & Lipman, D. J. (1990). Basic local alignment search tool. *Journal of Molecular Biology*, *215,* 403–410.

Andersen, B. G., Sejrup, H. P., & Kirkhus, O. (1983). Deposits at Bø on Karmøy, SW Norway. *Norges Geologiske Undersøkelser*, *380*, 189— 201.

Branco, S., Bi, K., Liao, H.-L., Gladieux, P., Badouin, H., Ellison, C. E., Nguyen, N. H., Vilgalys, R., Peay, K. G., Taylor, J. W., & Bruns, T. D. (2017). Continental-level population differentiation and environmental adaptation in the mushroom *Suillus brevipes*. *Molecular Ecology*, *26*(7), 2063–2076. https://doi.org/10.1111/mec.13892

Branco, S., Gladieux, P., Ellison, C. E., Kuo, A., LaButti, K., Lipzen, A., Grigoriev, I. V., Liao, H.-L., Vilgalys, R., Peay, K. G., Taylor, J. W., & Bruns, T. D. (2015). Genetic isolation between two recently diverged populations of a symbiotic fungus. *Molecular Ecology*, *24*(11), 2747–2758. https://doi.org/10.1111/mec.13132

Capblancq, T., Luu, K., Blum, M. G. B., & Bazin, E. (2018). Evaluation of redundancy analysis to identify signatures of local adaptation. *Molecular Ecology Resources*, *18*(6), 1223–1233. https://doi.org/10.1111/1755-0998.12906

Clausen, J., Keck, D. D., & Hiesey, W. M. (1941). Regional Differentiation in Plant Species. *The American Naturalist*, *75*(758), 231–250. https://doi.org/10.1086/280955

Crowther, T. W., Maynard, D. S., Crowther, T. R., Peccia, J., Smith, J. R., & Bradford, M. A. (2014). Untangling the fungal niche: The trait-based approach. *Frontiers in Microbiology*, *5*, 579-579 https://doi.org/10.3389/fmicb.2014.00579

Davis, M. B., & Shaw, R. G. (2001). Range shifts and adaptive responses to Quaternary climate change. *Science*, *292*(5517), 673–679.

Diez, J., Kauserud, H., Andrew, C., Heegaard, E., Krisai-Greilhuber, I., Senn-Irlet, B., Høiland, K., Egli, S., & Büntgen, U. (2020). Altitudinal upwards shifts in fungal fruiting in the Alps. *Proceedings of the Royal Society B: Biological Sciences*, *287*(1919), 20192348. https://doi.org/10.1098/rspb.2019.2348

Dormann, C. F., Elith, J., Bacher, S., Buchmann, C., Carl, G., Carré, G., Marquéz, J. R. G., Gruber, B., Lafourcade, B., Leitão, P. J., Münkemüller, T., McClean, C., Osborne, P. E., Reineking, B., Schröder, B., Skidmore, A. K., Zurell, D., & Lautenbach, S. (2013). Collinearity: A review of methods to deal with it and a simulation study evaluating their performance. *Ecography*, *36*,(1), 27–46. https://doi.org/10.1111/j.1600-0587.2012.07348.x

Duforet-Frebourg, N., Luu, K., Laval, G., Bazin, E., & Blum, M. G. B. (2016). Detecting genomic signatures of natural selection with Principal Component Analysis: Application to the 1000 genomes data. *Molecular Biology and Evolution*, *33*(4), 1082–1093. https://doi.org/10.1093/molbev/msv334

Ellison, C. E., Hall, C., Kowbel, D., Welch, J., Brem, R. B., Glass, N. L., & Taylor, J. W. (2011). Population genomics and local adaptation in wild isolates of a model microbial eukaryote. *Proceedings of the National Academy of Sciences of the United States of America*, *108*(7), 2831–2836. https://doi.org/10.1073/pnas.1014971108

Ewels, P., Magnusson, M., Lundin, S., & Käller, M. (2016). MultiQC: Summarize analysis results for multiple tools and samples in a single report. *Bioinformatics*, *32*(19), 3047–3048. https://doi.org/10.1093/bioinformatics/btw354

Fisher, R. A. (1930). *The genetical theory of natural selection*. Claredon Pr Oxford.

Forester, B. R., Lasky, J. R., Wagner, H. H., & Urban, D. L. (2018). Comparing methods for detecting multilocus adaptation with multivariate genotype–environment associations. *Molecular Ecology*, *27*(9), 2215–2233. https://doi.org/10.1111/mec.14584

Galante, T. E., Horton, T. R., & Swaney, D. P. (2011). 95 % of basidiospores fall within 1 m of the cap: A field-and modeling-based study. *Mycologia*, *103*(6), 1175–1183. https://doi.org/10.3852/10-388

Gibson, M. J. S., & Moyle, L. C. (2020). Regional differences in the abiotic environment contribute to genomic divergence within a wild tomato species. *Molecular Ecology*, *29*(12), 2204–2217. https://doi.org/10.1111/mec.15477

Giesecke, T., & Bennett, K. D. (2014). The Holocene spread of *Picea abies* (L) Karst. In Fennoscandia and adjacent areas. *Journal of Biogeography*, *32*, 1523–1548.

Gratwicke, B., Ross, H., Batista, A., Chaves, G., Crawford, A. J., Elizondo, L., Estrada, A., Evans, M., Garelle, D., Guerrel, J., Hertz, A., Hughey, M., Jaramillo, C. A., Klocke, B., Mandica, M., Medina, D., Richards-Zawacki, C. L., Ryan, M. J., Sosa-Bartuano, A., … Ibáñez, R. (2016). Evaluating the probability of avoiding disease-related extinctions of Panamanian amphibians through captive breeding programs. *Animal Conservation*, *19*(4), 324–336. https://doi.org/10.1111/acv.12249

Green, D. (1999). How Do Amphibians Go Extinct? *Redpath Museum, McGill University*.

Guisan, A., & Thuiller, W. (2005). Predicting species distribution: Offering more than simple habitat models. *Ecology Letters*, *8*(9), 993–1009. https://doi.org/10.1111/j.1461-0248.2005.00792.x

Hoffmann, A. A., & Sgrò, C. M. (2011). Climate change and evolutionary adaptation. *Nature*, *470*(7335), 479–485. https://doi.org/10.1038/nature09670

Hollander, M., & Wolfe, D. A. (1973). Nonparametric Statistical Methods. *New York: John Wiley & Sons.*, 185–194.

Horvath, P., Halvorsen, R., Stordal, F., Tallaksen, L. M., Tang, H., & Bryn, A. (2019). Distribution modelling of vegetation types based on area frame survey data. *Applied Vegetation Science*, *22*(4), 547–560. https://doi.org/10.1111/avsc.12451

Huntley, B., & Birks, H. J. B. (1984). B. Huntley & H. J. B. Birks: An atlas of past and present pollen maps for Europe: 0–13,000 years ago. *Antiquity*, *58*(223), 154–155. https://doi.org/10.1017/S0003598X00051814

Kardol, P., Cregger, M. A., Campany, C. E., & Classen, A. T. (2010). Soil ecosystem functioning under climate change: Plant species and community effects. *Ecology*, *91*(3), 767–781. https://doi.org/10.1890/09-0135.1

Kauserud, H., Heegaard, E., Buntgen, U., Halvorsen, R., Egli, S., Senn-Irlet, B., Krisai-Greilhuber, I., Damon, W., Sparks, T., Norden, J., Hoiland, K., Kirk, P., Semenov, M., Boddy, L., & Stenseth, N. C. (2012). Warming-induced shift in European mushroom fruiting phenology. *Proceedings of the National Academy of Sciences*, *109*(36), 14488–14493. https://doi.org/10.1073/pnas.1200789109

Kauserud, H., & Schumacher, T. (2003). Regional and local population structure of the pioneer wood-decay fungus *Trichaptum abietinum*. *Mycologia*, *95*(3), 416–425. https://doi.org/10.1080/15572536.2004.11833086

Kauserud, H., Stige, L. C., Vik, J. O., Okland, R. H., Hoiland, K., & Stenseth, N. Chr. (2008). Mushroom fruiting and climate change. *Proceedings of the National Academy of Sciences*, *105*(10), 3811–3814. https://doi.org/10.1073/pnas.0709037105

Kemp, D. B., Eichenseer, K., & Kiessling, W. (2015). Maximum rates of climate change are systematically underestimated in the geological record. *Nature Communications*, *6*(1), 8890. https://doi.org/10.1038/ncomms9890

Khan, A., & Rayner, G. D. (2003). Robustness to Non-Normality of Common Tests for the Many-Sample Location Problem. Journal of Applied Mathematics and Decision Sciences*, 7(4), 187–206*, 21.

Knaus, B. J., & Grünwald, N. J. (2017). vcfr: A package to manipulate and visualize variant call format data in R. *Molecular Ecology Resources*, *17*(1), 44–53. https://doi.org/10.1111/1755-0998.12549

Knut Harstveit. (2020). Kontinentalt klima in *Store norske leksikon*. http://snl.no/kontinentalt_klima

Krings, M., Dotzler, N., Galtier, J., & Taylor, T. N. (2011). Oldest fossil basidiomycete clamp connections. *Mycoscience*, *52*(1), 18–23. https://doi.org/10.1007/S10267-010-0065-4

Kronholm, I., Picó, F. X., Alonso-Blanco, C., Goudet, J., & Meaux, J. de. (2012). Genetic basis of adaptation in *Arabidopsis thaliana*: Local adaptation at the seed dormancy qtl Dog1. *Evolution*, *66*(7), 2287–2302. https://doi.org/10.1111/j.1558-5646.2012.01590.x

Kubota, S., Iwasaki, T., Hanada, K., Nagano, A. J., Fujiyama, A., Toyoda, A., Sugano, S., Suzuki, Y., Hikosaka, K., Ito, M., & Morinaga, S.-I. (2015). A genome scan for genes underlying microgeographic-scale local adaptation in a wild *Arabidopsis* species. *PLOS Genetics*, *11*(7), e1005361. https://doi.org/10.1371/journal.pgen.1005361

Legendre, P., & Legendre, L. (2012). *Numerical Ecology*. Elsevier.

Li, H., & Durbin, R. (2010). Fast and accurate long-read alignment with Burrows–Wheeler transform. *Bioinformatics*, *26*(5), 589–595.

Li, H., Handsaker, B., Wysoker, A., Fennell, T., Ruan, J., Homer, N., Marth, G., Abecasis, G., & Durbin, R. (2009). The sequence alignment/map format and SAMtools. *Bioinformatics*, *25*(16), 2078–2079. https://doi.org/10.1093/bioinformatics/btp352

Liu, C.-C., Shringarpure, S., Lange, K., & Novembre, J. (2020). Exploring population structure with admixture models and principal component analysis in *Statistical Population Genomics* (s. 67–86). Humana, New York, NY.

Liu, H. (2015). Comparing Welch's ANOVA, a Kruskal-Wallis test and traditional ANOVA in case of Heterogeneity of Variance. *Virginia Commonwealth University*, 48.

Lu, D. S. Inferring the origin of reproductive barriers in Trichaptum abietinum. *In prep*.

Lustenhouwer, N., Maynard, D. S., Bradford, M. A., Lindner, D. L., Oberle, B., Zanne, A. E., & Crowther, T. W. (2020). A trait-based understanding of wood decomposition by fungi. *Proceedings of the National Academy of Sciences of the United States of America*, *117*(21), 11551–11558. https://doi.org/10.1073/pnas.1909166117

Magan, N., & Lacey, J. (1984). Effect of water activity, temperature and substrate on interactions between field and storage fungi. *Transactions of the British Mycological Society*, *82*(1), 83–93. https://doi.org/10.1016/S0007-1536(84)80214-4

Mangerud, J., Sønstegaard, F., Sejrup, H.-P., & Haldorsen, S. (1981). A continuous Eemian-Early Weichselian sequence containing pollen and marine fossils at Fjøsanger, western Norwav. *Boreas*, *Vol. 10. pp.*(137-208.).

Martina, J. P., & von Ende, C. N. (2012). Highly plastic response in morphological and physiological traits to light, soil-N and moisture in the model invasive plant, *Phalaris arundinacea*. *Environmental and Experimental Botany*, *82*, 43–53. https://doi.org/10.1016/j.envexpbot.2012.03.010

Maynard, D. S., Bradford, M. A., Covey, K. R., Lindner, D., Glaeser, J., Talbert, D. A., Tinker, P. J., Walker, D. M., & Crowther, T. W. (2019). Consistent trade-offs in fungal trait expression across broad spatial scales. *Nature Microbiology*, *4*(5), 846–853. https://doi.org/10.1038/s41564-019-0361-5

O'Donnell, M.S., and Ignizio. (2012). Bioclimatic predictors for supporting ecological applications in the conterminous United States. *U.S. Geological Survey Data Series 691, 10 p.*

Ohlson, M., Brown, K. J., Birks, H. J. B., Grytnes, J.-A., Hörnberg, G., Niklasson, M., Seppä, H., & Bradshaw, R. H. W. (2011). Invasion of Norway spruce diversifies the fire regime in boreal European forests. *Journal of Ecology*, *99*(2), 395–403. https://doi.org/10.1111/j.1365-2745.2010.01780.x

Oksanen, J., Kindt, R., Legendre, P., Hara, B., Simpson, G., Solymos, P., Henry, M., Stevens, H., Maintainer, H. (2009). *The vegan Package*.

Olson-Manning, C. F., Wagner, M. R., & Mitchell-Olds, T. (2012). Adaptive evolution: Evaluating empirical support for theoretical predictions. *Nature Reviews Genetics*, *13*(12), 867–877. https://doi.org/10.1038/nrg3322

Parducci, L., Jorgensen, T., Tollefsrud, M. M., Elverland, E., Alm, T., Fontana, S. L., Bennett, K. D., Haile, J., Matetovici, I., Suyama, Y., Edwards, M. E., Andersen, K., Rasmussen, M., Boessenkool, S., Coissac, E., Brochmann, C., Taberlet, P., Houmark-Nielsen, M., Larsen, N. K., … Willerslev, E. (2012). Glacial survival of boreal trees in Northern Scandinavia. *Science*, *335*, 1083–1086. https://doi.org/10.1126/science.1216043

Patterson, N., Price, A. L., & Reich, D. (2006). Population structure and eigenanalysis. *PLOS Genetics*, *2*(12), e190. https://doi.org/10.1371/journal.pgen.0020190

Peay, K. G., Schubert, M. G., Nguyen, N. H., & Bruns, T. D. (2012). Measuring ectomycorrhizal fungal dispersal: Macroecological patterns driven by microscopic propagules. *Molecular Ecology*, *21*(16), 4122–4136. https://doi.org/10.1111/j.1365-294X.2012.05666.x

Pecl, G. T., Araújo, M. B., Bell, J. D., Blanchard, J., Bonebrake, T. C., Chen, I.-C., Clark, T. D., Colwell, R. K., Danielsen, F., Evengård, B., Falconi, L., Ferrier, S., Frusher, S., Garcia, R. A., Griffis, R. B., Hobday, A. J., Janion-Scheepers, C., Jarzyna, M. A., Jennings, S., … Williams,

S. E. (2017). Biodiversity redistribution under climate change: Impacts on ecosystems and human well-being. *Science*, *355,* 6332-6332. https://doi.org/10.1126/science.aai9214

Peris, D., Lu, D. S., Kinneberg, V. B., Methlie, I.-S., Dahl, M. S., Kauserud, H., & Skrede, I. (u.å.). Long-term balancing selection in two highly dynamic mating loci generates trans-species polymorphisms in fungi. *In prep*.

Peterson, M. L., Doak, D. F., & Morris, W. F. (2018). Both life-history plasticity and local adaptation will shape range-wide responses to climate warming in the tundra plant *Silene acaulis*. *Global Change Biology*, *24*(4), 1614–1625. https://doi.org/10.1111/gcb.13990

Petit, R. J., Bialozyt, R., Garnier-Géré, P., & Hampe, A. (2004). Ecology and genetics of tree invasions: From recent introductions to Quaternary migrations. *Forest Ecology and Management*, *197*(1–3), 117–137. https://doi.org/10.1016/j.foreco.2004.05.009

Petit, R. J., Brewer, S., Bordacs, S., Burg, K., Cheddadi, R., Coart, E., Cottrell, J., & Csaikl, U. M. (2002). Identification of refugia and post-glacial colonisation routes of European white oaks based on chloroplast DNA and fossil pollen evidence. *Forest Ecology and Management*, 156, 49-74.

Poplin, R., Ruano-Rubio, V., DePristo, M. A., Fennell, T. J., Carneiro, M. O., Auwera, G. A. V. der, Kling, D. E., Gauthier, L. D., Levy-Moonshine, A., Roazen, D., Shakir, K., Thibault, J., Chandran, S., Whelan, C., Lek, M., Gabriel, S., Daly, M. J., Neale, B., MacArthur, D. G., & Banks, E. (2018). Scaling accurate genetic variant discovery to tens of thousands of samples. *BioRxiv*, 201178. https://doi.org/10.1101/201178

Price, A. L., Patterson, N. J., Plenge, R. M., Weinblatt, M. E., Shadick, N. A., & Reich, D. (2006). Principal components analysis corrects for stratification in genome-wide association studies. *Nature Genetics*, *38*(8), 904–909. https://doi.org/10.1038/ng1847

Privé, F., Luu, K., Blum, M. G. B., McGrath, J. J., & Vilhjálmsson, B. J. (2020). Efficient toolkit implementing best practices for principal component analysis of population genetic data. *Bioinformatics*, *36*(16), 4449–4457. https://doi.org/10.1093/bioinformatics/btaa520

Purcell, J., Pirogan, D., Avril, A., Bouyarden, F., & Chapuisat, M. (2016). Environmental influence on the phenotype of ant workers revealed by common garden experiment. *Behavioral Ecology and Sociobiology*, *70*(3), 357–367. https://doi.org/10.1007/s00265-015-2055-1

Rellstab, C., Gugerli, F., Eckert, A. J., Hancock, A. M., & Holderegger, R. (2015). A practical guide to environmental association analysis in landscape genomics. *Molecular Ecology*, *24*(17), 4348–4370. https://doi.org/10.1111/mec.13322

Ropars, J., Maufrais, C., Diogo, D., Marcet-Houben, M., Perin, A., Sertour, N., Mosca, K., Permal, E., Laval, G., Bouchier, C., Ma, L., Schwartz, K., Voelz, K., May, R. C., Poulain, J., Battail, C., Wincker, P., Borman, A. M., Chowdhary, A., … d'Enfert, C. (2018). Gene flow contributes to diversification of the major fungal pathogen *Candida albicans*. *Nature Communications*, *9*(1), 2253. https://doi.org/10.1038/s41467-018-04787-4

Schimel, J., Balser, T. C., & Wallenstein, M. (2007). Microbial stress-response physiology and its implications for ecosystem function. *Ecology*, *88*(6), 1386–1394. https://doi.org/10.1890/06-0219

Seierstad, K. S., Fossdal, R., Miettinen, O., Carlsen, T., Skrede, I., & Kauserud, H. (2021). Contrasting genetic structuring in the closely related basidiomycetes *Trichaptum abietinum* and *Trichaptum fuscoviolaceum* (Hymenochaetales). *Fungal Biology*, *125*(4), 269–275. https://doi.org/10.1016/j.funbio.2020.11.001

Slatkin, M. (1987). Gene flow and the geographic structure of natural populations. *Science*, *236*(4803), 787–792.

Stuart, S. N., Chanson, J. S., Cox, N. A., Young, B. E., Rodrigues, A. S. L., Fischman, D. L., & Waller, R. W. (2004). Status and trends of amphibian declines and extinctions worldwide. *Science*, *306*(5702), 1783–1786. https://doi.org/10.1126/science.1103538

Tollefsrud, M. M., Latałowa, M., Knaap, W. O. van der, Brochmann, C., & Sperisen, C. (2015). Late Quaternary history of North Eurasian Norway spruce (*Picea abies*) and Siberian spruce (*Picea obovata*) inferred from macrofossils, pollen and cytoplasmic DNA variation. *Journal of Biogeography*, *42*(8), 1431–1442. https://doi.org/10.1111/jbi.12484

Tomczak, M., & Tomczak, E. (2014). The need to report effect size estimates revisited. An overview of some recommended measures of effect size. Trends in Sport Sciences *1*(21), 19–25.

Treseder, K. K., & Lennon, J. T. (2015). Fungal traits that drive ecosystem dynamics on land. *Microbiology and Molecular Biology Reviews*, *79*(2), 243–262. https://doi.org/10.1128/MMBR.00001-15

Van der Auwera GA & O'Connor BD. (2020). *Genomics in the Cloud: Using Docker, GATK, and WDL in Terra 1st Edition*.

Vorren, T. O., & Mangerud, J. (2006). Mellomistider avsløres på land». I I.B. Ramberg, I. Bryhni og A. Nøttvedt. Landet blir til: Norges geologi. . . *Landet blir til: Norges geologi. Trondheim: Norsk Geologisk Forening.*, 498–500.

White, TJ., Bruns, T., Lee, T., & Taylor, J. (1990). Amplification and direct sequencing of fungal ribosomal RNA genes for phylogenetics. PCR Protocols: A Guide to Methods and Applications. *New York: Academic Press Inc*, 315–322.

Wickham, H. (2019). *stringr: Simple, Consistent Wrappers for Common String Operations* (1.4.0) [R package version 1.4.0]. https://CRAN.R-project.org/package=stringr

Williams, G. C. (1996). *Adaptation and natural selection: A critique of some current evolutionary thought*. Princeton Univ. Press.

Øyen, B.-H. (2017). *Spontan og plantet gran på Vestlandet og i Nord-Norge* (Kystskogbruket, s. 36) [Rapport 1/17]. Skognæring Kyst S/A

Supplementary

a)

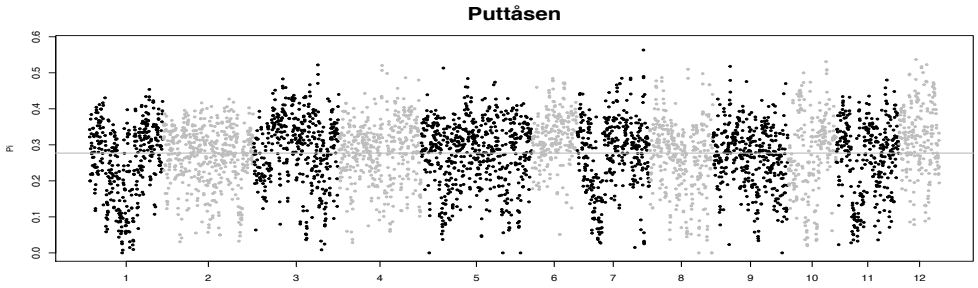

b)

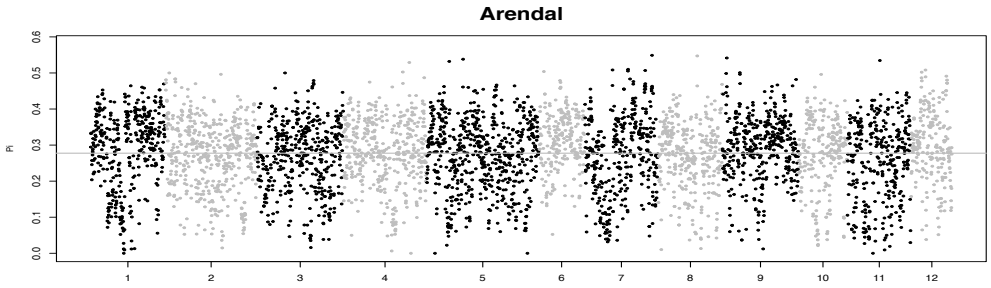

c)

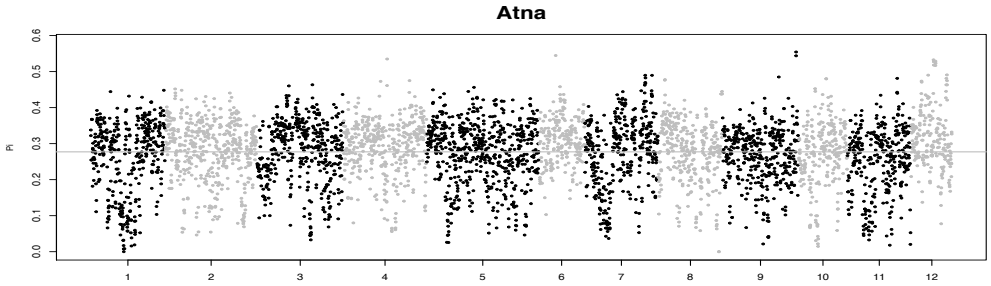

d)

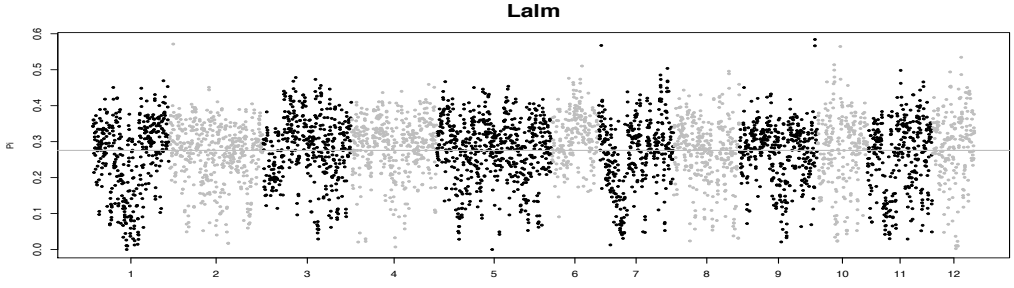

e)

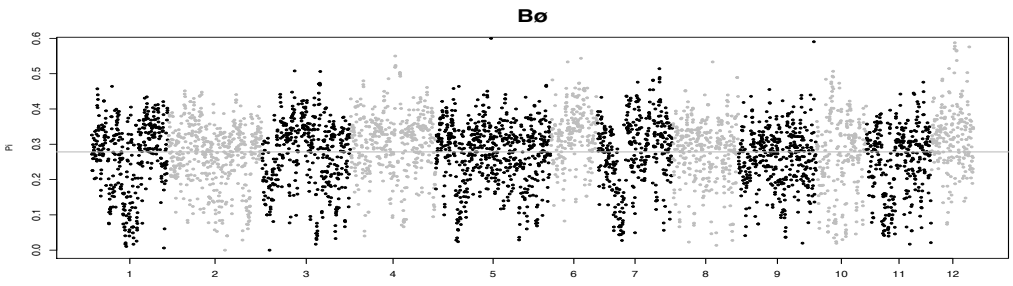

f)

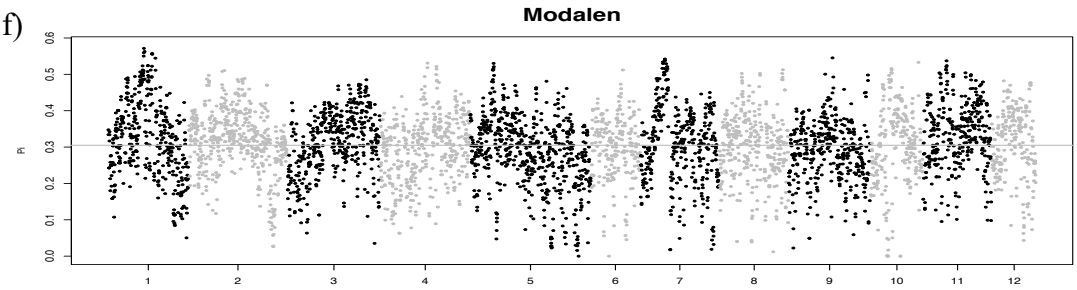

Figure S1: Scatter plots from sliding window genome scans of Pi, using a SNP dataset of 1,163,262 SNPs, for all populations a-f. Each plot represents Pi for one sliding window (20 kb) from the genome scan. Scaffolds, from 1-12, are illustrated along the x-axis, while the y-axis represents the pi value, ranging from 0-1. The horizontal line marks the mean value.

Table S1: Overview of genes found in positions of 266 significant SNPs identified by RDA to correlate with Annual Precipitation (Bioclim 12) and Isothermality (Bioclim 3). The columns describe: Genomic location, Predictor variable, Correlation coefficient, Gene info and Gene notes.

Genomic location	Predictor	Correlation	Gene_info	Gene_Note
Scaffold01_3529720	bioclim_12	0,835492909	maker-Scaffold01-augustus-gene-35.47/maker-Scaffold01-augustus-gene-35.3/"mitochondrial 50S ribosomal protein L3"	"Similar to BCS1: Mitochondrial chaperone BCS1 (Saccharomyces cerevisiae (strain ATCC 204508 / S288c) OX=559292)"/"Similar to Glycylpeptide N-tetradecanoyltransferase (Cryptococcus neoformans OX=5207)"
Scaffold02_3531159	bioclim_12	0,86033947	maker-Scaffold02-snap-gene-35.95	"Similar to Glycine-rich RNA-binding protein GRP1A (Sinapis alba OX=3728)"
Scaffold02_4367140	bioclim_12	0,923108221	maker-Scaffold02-augustus-gene-43.76/"predicted protein"	"Similar to CHS3: Chitin synthase 3 (Cryptococcus neoformans var. grubii serotype A (strain H99 / ATCC 208821 / CBS 10515 / FGSC 9487) OX=235443)"
Scaffold02_4394020	bioclim_12	0,968920595	genemark-Scaffold02-processed-gene-44.0/maker-Scaffold02-augustus-gene-44.19	"Similar to NDC80: Probable kinetochore protein NDC80 (Cryptococcus neoformans var. neoformans serotype D (strain JEC21 / ATCC MYA-565) OX=214684)"/"Similar to copb1: Coatomer subunit beta (Danio rerio OX=7955)"
Scaffold02_4401807	bioclim_12	0,968920595	maker-Scaffold02-augustus-gene-44.19/"Coatomer subunit beta"	"Similar to copb1: Coatomer subunit beta (Danio rerio OX=7955)"
Scaffold02_4403477	bioclim_12	0,84748488	maker-Scaffold02-augustus-gene-44.19	"Similar to copb1: Coatomer subunit beta (Danio rerio OX=7955)"
Scaffold02_4403757	bioclim_12	0,968920595	maker-Scaffold02-augustus-gene-44.19	"Similar to copb1: Coatomer subunit beta (Danio rerio OX=7955)"
Scaffold02_4403838	bioclim_12	0,968920595	maker-Scaffold02-augustus-gene-44.19	"Similar to copb1: Coatomer subunit beta (Danio rerio OX=7955)"
Scaffold02_4403865	bioclim_12	0,968920595	maker-Scaffold02-augustus-gene-44.19	"Similar to copb1: Coatomer subunit beta (Danio rerio OX=7955)"

Scaffold02_4404316	bioclim_12	0,968920595	maker-Scaffold02-augustus-gene-44.19	"Similar to copb1: Coatomer subunit beta (Danio rerio OX=7955)"
Scaffold02_4405076	bioclim_12	0,968920595	maker-Scaffold02-augustus-gene-44.19	"Similar to copb1: Coatomer subunit beta (Danio rerio OX=7955)"
Scaffold02_4413215	bioclim_12	0,968920595	snap_masked-Scaffold02-abinit-gene-44.17	"Similar to SSN3: Serine/threonine-protein kinase SSN3 (Kluyveromyces lactis (strain ATCC 8585 / CBS 2359 / DSM 70799 / NBRC 1267 / NRRL Y-1140 / WM37) OX=284590)"
Scaffold02_4413278	bioclim_12	0,968920595	snap_masked-Scaffold02-abinit-gene-44.17	"Similar to SSN3: Serine/threonine-protein kinase SSN3 (Kluyveromyces lactis (strain ATCC 8585 / CBS 2359 / DSM 70799 / NBRC 1267 / NRRL Y-1140 / WM37) OX=284590)"
Scaffold02_4417618	bioclim_12	0,968920595	maker-Scaffold02-augustus-gene-44.30	"Similar to SMC4: Structural maintenance of chromosomes protein 4 (Saccharomyces cerevisiae (strain ATCC 204508 / S288c) OX=559292)"
Scaffold02_4417916	bioclim_12	0,968920595	maker-Scaffold02-augustus-gene-44.30	"Similar to SMC4: Structural maintenance of chromosomes protein 4 (Saccharomyces cerevisiae (strain ATCC 204508 / S288c) OX=559292)"
Scaffold02_4482974	bioclim_12	0,883816801	maker-Scaffold02-snap-gene-44.9	"Protein of unknown function"
Scaffold02_4483555	bioclim_12	0,883816801	maker-Scaffold02-snap-gene-44.9	"Protein of unknown function"
Scaffold02_4484056	bioclim_12	0,883816801	maker-Scaffold02-snap-gene-44.9	"Protein of unknown function"
Scaffold02_4484226	bioclim_12	0,84748488	maker-Scaffold02-snap-gene-44.9	"Protein of unknown function"
Scaffold02_4491225	bioclim_12	0,968920595	maker-Scaffold02-exonerate_protein2genome-gene-45.143/maker-Scaffold02-snap-gene-45.1	"Similar to SNF1: Carbon catabolite-derepressing protein kinase (Saccharomyces cerevisiae) (strain ATCC 204508 / S288c) OX=559292)"

Scaffold02_4516328	bioclim_12	0,88060645	maker-Scaffold02-snap-gene-45.6	"Similar to exo5: Probable exonuclease V, mitochondrial (Schizosaccharomyces pombe (strain 972 / ATCC 24843) OX=284812)"
Scaffold02_4516403	bioclim_12	0,88060645	maker-Scaffold02-snap-gene-45.6	"Similar to exo5: Probable exonuclease V, mitochondrial (Schizosaccharomyces pombe (strain 972 / ATCC 24843) OX=284812)"
Scaffold02_4516769	bioclim_12	0,968920595	maker-Scaffold02-snap-gene-45.6	"Similar to exo5: Probable exonuclease V, mitochondrial (Schizosaccharomyces pombe (strain 972 / ATCC 24843) OX=284812)"
Scaffold02_4527394	bioclim_12	0,968920595	maker-Scaffold02-snap-gene-45.27	"Similar to sidH: Mevalonyl-coenzyme A hydratase sidH (Neosartorya fumigata (strain ATCC MYA-4609 / Af293 / CBS 101355 / FGSC A1100) OX=330879)"
Scaffold02_4530550	bioclim_12	0,968920595		
Scaffold02_4531298	bioclim_12	0,968920595		
Scaffold02_4541031	bioclim_12	0,906371134		
Scaffold02_4561247	bioclim_12	0,968920595	maker-Scaffold02-augustus-gene-45.78	"Similar to faeB-2: Probable feruloyl esterase B-2 (Aspergillus oryzae (strain ATCC 42149 / RIB 40) OX=510516)"
Scaffold02_4561307	bioclim_12	0,968920595	maker-Scaffold02-augustus-gene-45.78	"Similar to faeB-2: Probable feruloyl esterase B-2 (Aspergillus oryzae (strain ATCC 42149 / RIB 40) OX=510516)"
Scaffold02_4565339	bioclim_12	0,923108221	maker-Scaffold02-augustus-gene-45.78	"Similar to faeB-2: Probable feruloyl esterase B-2 (Aspergillus oryzae (strain ATCC 42149 / RIB 40) OX=510516)"
Scaffold02_4565816	bioclim_12	0,923108221	maker-Scaffold02-augustus-gene-45.78	"Similar to faeB-2: Probable feruloyl esterase B-2 (Aspergillus oryzae (strain ATCC 42149 / RIB 40) OX=510516)"
Scaffold02_4565838	bioclim_12	0,923108221	maker-Scaffold02-augustus-gene-45.78	"Similar to faeB-2: Probable feruloyl esterase B-2 (Aspergillus oryzae (strain ATCC 42149 / RIB 40) OX=510516)"
Scaffold02_4566726	bioclim_12	0,923108221	maker-Scaffold02-augustus-gene-45.78	"Similar to faeB-2: Probable feruloyl esterase B-2 (Aspergillus oryzae (strain ATCC 42149 / RIB 40) OX=510516)"
Scaffold02_4567642	bioclim_12	0,923108221		

Scaffold02_4569144	bioclim_12	0,906371134	maker-Scaffold02-augustus-gene-45.70/"ARM repeat-containing protein"	"Similar to SPBC1703.03c: Uncharacterized ARM-like repeat-containing protein C1703.03c (Schizosaccharomyces pombe (strain 972 / ATCC 24843) OX=284812)"
Scaffold02_4569310	bioclim_12	0,906371134	maker-Scaffold02-augustus-gene-45.70/"ARM repeat-containing protein"	"Similar to SPBC1703.03c: Uncharacterized ARM-like repeat-containing protein C1703.03c (Schizosaccharomyces pombe (strain 972 / ATCC 24843) OX=284812)"
Scaffold02_4610640	bioclim_12	0,88060645	maker-Scaffold02-augustus-gene-46.28/"AP-3 complex subunit delta"	"Similar to Ap3d1: AP-3 complex subunit delta-1 (Mus musculus OX=10090)"
Scaffold03_3024238	bioclim_12	0,892504127	maker-Scaffold03-augustus-gene-30.34/maker-Scaffold03-augustus-gene-30.34	"Similar to KLF11: Krueppel-like factor 11 (Homo sapiens OX=9606)"/"Similar to KLF11: Krueppel-like factor 11 (Homo sapiens OX=9606)"
Scaffold03_3024289	bioclim_12	0,892504127	maker-Scaffold03-augustus-gene-30.34/maker-Scaffold03-augustus-gene-30.34	"Similar to KLF11: Krueppel-like factor 11 (Homo sapiens OX=9606)"/"Similar to KLF11: Krueppel-like factor 11 (Homo sapiens OX=9606)"
Scaffold03_3024537	bioclim_12	0,892504127	maker-Scaffold03-augustus-gene-30.34/maker-Scaffold03-augustus-gene-30.34	"Similar to KLF11: Krueppel-like factor 11 (Homo sapiens OX=9606)"/"Similar to KLF11: Krueppel-like factor 11 (Homo sapiens OX=9606)"
Scaffold03_3025596	bioclim_12	0,892504127	maker-Scaffold03-augustus-gene-30.34/maker-Scaffold03-augustus-gene-30.34/"ferredoxin reductase-like protein"	"Similar to KLF11: Krueppel-like factor 11 (Homo sapiens OX=9606)"/"Similar to KLF11: Krueppel-like factor 11 (Homo sapiens OX=9606)"
Scaffold03_3026797	bioclim_12	0,892504127	maker-Scaffold03-augustus-gene-30.34/"ferredoxin reductase-like	"Similar to KLF11: Krueppel-like factor 11 (Homo sapiens OX=9606)"/"Similar to KLF11: Krueppel-like factor 11 (Homo sapiens OX=9606)"

			protein"/"phenylalanine-tRNA ligase"	
Scaffold03_3028022	bioclim_12	0,892504127	maker-Scaffold03-augustus-gene-30.34/"ferredoxin reductase-like protein"/"phenylalanine-tRNA ligase"	"Similar to KLF11: Krueppel-like factor 11 (Homo sapiens OX=9606)"/"Similar to KLF11: Krueppel-like factor 11 (Homo sapiens OX=9606)"
Scaffold03_3030076	bioclim_12	0,892504127	snap_masked-Scaffold03-processed-gene-30.46/"snare protein syntaxin 18/UFE1"	"Similar to STX18: Syntaxin-18 (Homo sapiens OX=9606)"/"Similar to STX18: Syntaxin-18 (Homo sapiens OX=9606)"
Scaffold03_3033977	bioclim_12	0,892504127	maker-Scaffold03-augustus-gene-30.35/maker-Scaffold03-augustus-gene-30.35	"Similar to FRS1: Phenylalanine--tRNA ligase beta subunit (S+E46yces cerevisiae (strain ATCC 204508 / S288c) OX=559292)"/"Similar to FRS1: Phenylalanine--tRNA ligase beta subunit (Saccharomyces cerevisiae (strain ATCC 204508 / S288c) OX=559292)"
Scaffold03_3035399	bioclim_12	0,892504127		
Scaffold03_3038676	bioclim_12	0,892504127	snap_masked-Scaffold03-processed-gene-30.47/"Diphthine--ammonia ligase"	"Similar to mug71: Diphthine--ammonia ligase (Schizosaccharomyces pombe (strain 972 / ATCC 24843) OX=284812)"/"Similar to mug71: Diphthine--ammonia ligase (Schizosaccharomyces pombe (strain 972 / ATCC 24843) OX=284812)"
Scaffold03_3040754	bioclim_12	0,892504127	snap_masked-Scaffold03-abinit-gene-30.44/"MFS general substrate transporter"	"Similar to sut1: General alpha-glucoside permease (Schizosaccharomyces pombe (strain 972 / ATCC 24843) OX=284812)"/"Similar to sut1: General alpha-glucoside permease (Schizosaccharomyces pombe (strain 972 / ATCC 24843) OX=284812)"
Scaffold03_3045673	bioclim_12	0,892504127	snap_masked-Scaffold03-abinit-gene-30.32/snap_masked-	"Similar to FRS1: Phenylalanine--tRNA ligase beta subunit (Saccharomyces cerevisiae (strain ATCC 204508 / S288c) OX=559292)"/"Similar to FRS1: Phenylalanine--tRNA ligase beta

			Scaffold03-abinit-gene-30.32/"phenylalanyl-tRNA synthetase"	subunit (Saccharomyces cerevisiae (strain ATCC 204508 / S288c) OX=559292)"
Scaffold03_3046908	bioclim_12	0,892504127	snap_masked-Scaffold03-abinit-gene-30.32/snap_masked-Scaffold03-abinit-gene-30.32/"phenylalanyl-tRNA synthetase"	"Similar to FRS1: Phenylalanine--tRNA ligase beta subunit (Saccharomyces cerevisiae (strain ATCC 204508 / S288c) OX=559292)"/"Similar to FRS1: Phenylalanine--tRNA ligase beta subunit (Saccharomyces cerevisiae (strain ATCC 204508 / S288c) OX=559292)"
Scaffold03_3048846	bioclim_12	0,892504127	snap_masked-Scaffold03-abinit-gene-30.32/snap_masked-Scaffold03-abinit-gene-30.32	"Similar to FRS1: Phenylalanine--tRNA ligase beta subunit (Saccharomyces cerevisiae (strain ATCC 204508 / S288c) OX=559292)"/"Similar to FRS1: Phenylalanine--tRNA ligase beta subunit (Saccharomyces cerevisiae (strain ATCC 204508 / S288c) OX=559292)"
Scaffold03_3050725	bioclim_12	0,892504127	snap_masked-Scaffold03-processed-gene-30.51/snap_masked-Scaffold03-processed-gene-30.51	"Protein of unknown function"/"Protein of unknown function"
Scaffold03_3057237	bioclim_12	0,892504127	maker-Scaffold03-snap-gene-30.12/genemark-Scaffold03-processed-gene-30.27/maker-Scaffold03-snap-gene-30.12/	"Protein of unknown function"/"Protein of unknown function"/"Protein of unknown function"/"Protein of unknown function"
Scaffold03_3058181	bioclim_12	0,892504127	maker-Scaffold03-exonerate_est2genome-gene-30.215/maker-Scaffold03-exonerate_est2genome-gene-30.215	"Protein of unknown function"/"Protein of unknown function"

Scaffold03_3060739	bioclim_12	0,892504127	snap_masked-Scaffold03-processed-gene-31.43/snap_masked-Scaffold03-processed-gene-30.62	"Protein of unknown function"/"Similar to ZNHIT6: Box C/D snoRNA protein 1 (Pongo abelii OX=9601)"/"Protein of unknown function"/"Similar to ZNHIT6: Box C/D snoRNA protein 1 (Pongo abelii OX=9601)"
Scaffold03_3061417	bioclim_12	0,892504127	snap_masked-Scaffold03-processed-gene-31.43/snap_masked-Scaffold03-processed-gene-30.62	"Protein of unknown function"/"Similar to ZNHIT6: Box C/D snoRNA protein 1 (Pongo abelii OX=9601)"/"Protein of unknown function"/"Similar to ZNHIT6: Box C/D snoRNA protein 1 (Pongo abelii OX=9601)"
Scaffold03_3062285	bioclim_12	0,892504127	maker-Scaffold03-augustus-gene-31.50/maker-Scaffold03-augustus-gene-31.50	"Similar to sck1: Serine/threonine-protein kinase sck1 (Schizosaccharomyces pombe (strain 972 / ATCC 24843) OX=284812)"/"Similar to sck1: Serine/threonine-protein kinase sck1 (Schizosaccharomyces pombe (strain 972 / ATCC 24843) OX=284812)"
Scaffold03_3065221	bioclim_12	0,892504127	maker-Scaffold03-snap-gene-30.24/maker-Scaffold03-augustus-gene-31.50/maker-Scaffold03-snap-gene-30.24/	"Protein of unknown function"/"Similar to sck1: Serine/threonine-protein kinase sck1 (Schizosaccharomyces pombe (strain 972 / ATCC 24843) OX=284812)"/"Protein of unknown function"/"Similar to sck1: Serine/threonine-protein kinase sck1 (Schizosaccharomyces pombe (strain 972 / ATCC 24843) OX=284812)"
Scaffold03_3070574	bioclim_12	0,892504127	maker-Scaffold03-augustus-gene-31.50/maker-Scaffold03-augustus-gene-31.50	"Similar to sck1: Serine/threonine-protein kinase sck1 (Schizosaccharomyces pombe (strain 972 / ATCC 24843) OX=284812)"/"Similar to sck1: Serine/threonine-protein kinase sck1 (Schizosaccharomyces pombe (strain 972 / ATCC 24843) OX=284812)"
Scaffold03_3071020	bioclim_12	0,892504127	maker-Scaffold03-augustus-gene-31.50/maker-Scaffold03-augustus-gene-31.50	"Similar to sck1: Serine/threonine-protein kinase sck1 (Schizosaccharomyces pombe (strain 972 / ATCC 24843) OX=284812)"/"Similar to sck1: Serine/threonine-protein kinase

				sck1 (Schizosaccharomyces pombe (strain 972 / ATCC 24843) OX=284812)"
Scaffold03_3071957	bioclim_12	0,892504127	maker-Scaffold03-snap-gene-30.26/maker-Scaffold03-augustus-gene-31.50/maker-Scaffold03-augustus-gene-31.50	"Similar to AIM32: Altered inheritance of mitochondria protein 32 (Clavispora lusitaniae (strain ATCC 42720) OX=306902)" (Schizosaccharomyces pombe (strain 972 / ATCC 24843) OX=284812)"/"Similar to AIM32: Altered inheritance of mitochondria protein 32
Scaffold03_3072519	bioclim_12	0,892504127	maker-Scaffold03-snap-gene-30.26/maker-Scaffold03-augustus-gene-31.50/maker-Scaffold03-augustus-gene-31.50	"Similar to AIM32: Altered inheritance of mitochondria protein 32 (Clavispora lusitaniae (strain ATCC 42720) OX=306902)" (Schizosaccharomyces pombe (strain 972 / ATCC 24843) OX=284812)"/"Similar to AIM32: Altered inheritance of mitochondria protein 32
Scaffold03_3072552	bioclim_12	0,892504127	maker-Scaffold03-snap-gene-30.26/maker-Scaffold03-augustus-gene-31.50/maker-Scaffold03-augustus-gene-31.50	"Similar to AIM32: Altered inheritance of mitochondria protein 32 (Clavispora lusitaniae (strain ATCC 42720) OX=306902)" (Schizosaccharomyces pombe (strain 972 / ATCC 24843) OX=284812)"/"Similar to AIM32: Altered inheritance of mitochondria protein 32
Scaffold03_3073371	bioclim_12	0,892504127	maker-Scaffold03-snap-gene-30.26/maker-Scaffold03-augustus-gene-31.50/maker-Scaffold03-augustus-gene-31.50	"Similar to AIM32: Altered inheritance of mitochondria protein 32 (Clavispora lusitaniae (strain ATCC 42720) OX=306902)" (Schizosaccharomyces pombe (strain 972 / ATCC 24843) OX=284812)"/"Similar to AIM32: Altered inheritance of mitochondria protein 32
Scaffold03_3075526	bioclim_12	0,892504127	maker-Scaffold03-augustus-gene-31.50/maker-Scaffold03-augustus-gene-31.50/"Mov34-domain-containing protein"	"Similar to sck1: Serine/threonine-protein kinase sck1 (Schizosaccharomyces pombe (strain 972 / ATCC 24843) OX=284812)"/"Similar to sck1: Serine/threonine-protein kinase sck1 (Schizosaccharomyces pombe (strain 972 / ATCC 24843) OX=284812)"
Scaffold03_3077241	bioclim_12	0,892504127	maker-Scaffold03-snap-gene-30.27/maker-Scaffold03-augustus-gene-	"Similar to rps18: 30S ribosomal protein S18, chloroplastic (Nymphaea alba OX=34301)"

			31.50/maker-Scaffold03-snap-gene-30.27/	
Scaffold03_3085991	bioclim_12	0,892504127	maker-Scaffold03-augustus-gene-31.50/maker-Scaffold03-augustus-gene-31.50	"Similar to sck1: Serine/threonine-protein kinase sck1 (Schizosaccharomyces pombe (strain 972 / ATCC 24843) OX=284812)"/"Similar to sck1: Serine/threonine-protein kinase sck1 (Schizosaccharomyces pombe (strain 972 / ATCC 24843) OX=284812)"
Scaffold03_3086569	bioclim_12	0,892504127	maker-Scaffold03-augustus-gene-31.50/maker-Scaffold03-augustus-gene-31.50/"Cellular morphogenesis-related protein"	"Similar to sck1: Serine/threonine-protein kinase sck1 (Schizosaccharomyces pombe (strain 972 / ATCC 24843) OX=284812)"/"Similar to sck1: Serine/threonine-protein kinase sck1 (Schizosaccharomyces pombe (strain 972 / ATCC 24843) OX=284812)"
Scaffold03_3087951	bioclim_12	0,892504127	maker-Scaffold03-augustus-gene-31.50/maker-Scaffold03-augustus-gene-31.50/"Cellular morphogenesis-related protein"	"Similar to sck1: Serine/threonine-protein kinase sck1 (Schizosaccharomyces pombe (strain 972 / ATCC 24843) OX=284812)"/"Similar to sck1: Serine/threonine-protein kinase sck1 (Schizosaccharomyces pombe (strain 972 / ATCC 24843) OX=284812)"
Scaffold03_3091046	bioclim_12	0,892504127	maker-Scaffold03-snap-gene-31.25/maker-Scaffold03-augustus-gene-31.50/"Cellular morphogenesis-related protein"	"Similar to EFR3: Protein EFR3 (Cryptococcus neoformans var. neoformans serotype D (strain JEC21 / ATCC MYA-565) OX=214684)"/"Similar to sck1: Serine/threonine-protein kinase sck1 (Schizosaccharomyces pombe (strain 972 / ATCC 24843) OX=284812)"
Scaffold03_3091126	bioclim_12	0,892504127	maker-Scaffold03-snap-gene-31.25/maker-Scaffold03-augustus-gene-31.50/"Cellular	"Similar to EFR3: Protein EFR3 (Cryptococcus neoformans var. neoformans serotype D (strain JEC21 / ATCC MYA-565) OX=214684)"/"Similar to sck1: Serine/threonine-protein kinase sck1 (Schizosaccharomyces pombe (strain 972 / ATCC 24843) OX=284812)"

			morphogenesis-related protein"	
Scaffold03_3091951	bioclim_12	0,892504127	maker-Scaffold03-snap-gene-31.25/maker-Scaffold03-augustus-gene-31.50/"Cellular morphogenesis-related protein"	"Similar to EFR3: Protein EFR3 (Cryptococcus neoformans var. neoformans serotype D (strain JEC21 / ATCC MYA-565) OX=214684)"/"Similar to sck1: Serine/threonine-protein kinase sck1 (Schizosaccharomyces pombe (strain 972 / ATCC 24843) OX=284812)"
Scaffold03_3092350	bioclim_12	0,892504127	maker-Scaffold03-snap-gene-31.25/maker-Scaffold03-augustus-gene-31.50/"Cellular morphogenesis-related protein"	"Similar to EFR3: Protein EFR3 (Cryptococcus neoformans var. neoformans serotype D (strain JEC21 / ATCC MYA-565) OX=214684)"/"Similar to sck1: Serine/threonine-protein kinase sck1 (Schizosaccharomyces pombe (strain 972 / ATCC 24843) OX=284812)"
Scaffold03_4101371	bioclim_12	0,84438893	"Myb-like domain"	
Scaffold03_4265844	biocklim_3	0,842877862	maker-Scaffold03-snap-gene-42.63/maker-Scaffold03-snap-gene-42.51/maker-Scaffold03-snap-gene-42.51	"Protein of unknown function"/"Similar to CYP6: Peptidyl-prolyl cis-trans isomerase-like 4 (Cryptococcus neoformans var. neoformans serotype D (strain JEC21 / ATCC MYA-565) OX=214684)"/"Protein of unknown function"
Scaffold03_4845277	bioclim_12	0,806497657	maker-Scaffold03-snap-gene-48.9/maker-Scaffold03-snap-gene-48.9	"Similar to nps10: Adenylate-forming reductase Nps10 (Heterobasidion annosum OX=13563)"
Scaffold03_4845279	bioclim_12	0,806497657	maker-Scaffold03-snap-gene-48.9/maker-Scaffold03-snap-gene-48.9	"Similar to nps10: Adenylate-forming reductase Nps10 (Heterobasidion annosum OX=13563)"/"Similar to nps10: Adenylate-forming reductase Nps10 (Heterobasidion annosum OX=13563)"
Scaffold03_4845298	bioclim_12	0,806497657	maker-Scaffold03-snap-gene-48.9/maker-Scaffold03-snap-gene-48.9	"Similar to nps10: Adenylate-forming reductase Nps10 (Heterobasidion annosum OX=13563)"/"Similar to nps10:

				Adenylate-forming reductase Nps10 (Heterobasidion annosum OX=13563)"
Scaffold03_4845910	bioclim_12	0,806497657	maker-Scaffold03-snap-gene-48.9/maker-Scaffold03-snap-gene-48.9	"Similar to nps10: Adenylate-forming reductase Nps10 (Heterobasidion annosum OX=13563)"/"Similar to nps10: Adenylate-forming reductase Nps10 (Heterobasidion annosum OX=13563)"
Scaffold03_4847320	bioclim_12	0,806497657	maker-Scaffold03-snap-gene-48.9/maker-Scaffold03-snap-gene-48.9	"Similar to nps10: Adenylate-forming reductase Nps10 (Heterobasidion annosum OX=13563)"/"Similar to nps10: Adenylate-forming reductase Nps10 (Heterobasidion annosum OX=13563)"
Scaffold03_4857289	bioclim_12	0,88060645	maker-Scaffold03-snap-gene-48.28/maker-Scaffold03-snap-gene-48.28	"Similar to nps10: Adenylate-forming reductase Nps10 (Heterobasidion annosum OX=13563)"/"Similar to nps10: Adenylate-forming reductase Nps10 (Heterobasidion annosum OX=13563)"
Scaffold04_839645	bioclim_12	0,892504127		
Scaffold04_840178	bioclim_12	0,892504127		
Scaffold05_1386855	bioclim_12	0,968920595	maker-Scaffold05-augustus-gene-13.66/maker-Scaffold05-augustus-gene-13.66	"Similar to PGN1: Polygalacturonase (Cochliobolus carbonum OX=5017)"/"Similar to PGN1: Polygalacturonase (Cochliobolus carbonum OX=5017)"
Scaffold05_1404543	bioclim_12	0,968920595	maker-Scaffold05-augustus-gene-14.12/maker-Scaffold05-augustus-gene-14.12	"Similar to acuE: Malate synthase, glyoxysomal (Emericella nidulans (strain FGSC A4 / ATCC 38163 / CBS 112.46 / NRRL 194 / M139) OX=227321)"/"Similar to acuE: Malate synthase, glyoxysomal (Emericella nidulans (strain FGSC A4 / ATCC 38163 / CBS 112.46 / NRRL 194 / M139) OX=227321)"
Scaffold05_1412779	bioclim_12	0,968920595	maker-Scaffold05-augustus-gene-14.32/maker-Scaffold05-augustus-gene-14.32	"Similar to Afg1l: AFG1-like ATPase (Mus musculus OX=10090)"/"Similar to Afg1l: AFG1-like ATPase (Mus musculus OX=10090)"

Scaffold05_1419993	bioclim_12	0,968920595	maker-Scaffold05-augustus-gene-14.32/maker-Scaffold05-augustus-gene-14.32	"Similar to Afg1l: AFG1-like ATPase (Mus musculus OX=10090)"/"Similar to Afg1l: AFG1-like ATPase (Mus musculus OX=10090)"
Scaffold05_1419995	bioclim_12	0,968920595	maker-Scaffold05-augustus-gene-14.32/maker-Scaffold05-augustus-gene-14.32	"Similar to Afg1l: AFG1-like ATPase (Mus musculus OX=10090)"/"Similar to Afg1l: AFG1-like ATPase (Mus musculus OX=10090)"
Scaffold05_1420130	bioclim_12	0,968920595	maker-Scaffold05-augustus-gene-14.32/maker-Scaffold05-augustus-gene-14.32	"Similar to Afg1l: AFG1-like ATPase (Mus musculus OX=10090)"/"Similar to Afg1l: AFG1-like ATPase (Mus musculus OX=10090)"
Scaffold05_1420198	bioclim_12	0,968920595	maker-Scaffold05-augustus-gene-14.32/maker-Scaffold05-augustus-gene-14.32	"Similar to Afg1l: AFG1-like ATPase (Mus musculus OX=10090)"/"Similar to Afg1l: AFG1-like ATPase (Mus musculus OX=10090)"
Scaffold05_1421480	bioclim_12	0,892504127	maker-Scaffold05-augustus-gene-14.32/maker-Scaffold05-augustus-gene-14.32	"Similar to Afg1l: AFG1-like ATPase (Mus musculus OX=10090)"/"Similar to Afg1l: AFG1-like ATPase (Mus musculus OX=10090)"
Scaffold05_1425253	bioclim_12	0,968920595	maker-Scaffold05-augustus-gene-14.32/maker-Scaffold05-augustus-gene-14.32	"Similar to Afg1l: AFG1-like ATPase (Mus musculus OX=10090)"/"Similar to Afg1l: AFG1-like ATPase (Mus musculus OX=10090)"
Scaffold05_1430123	bioclim_12	0,883816801		
Scaffold05_1431931	bioclim_12	0,968920595	maker-Scaffold05-exonerate_protein2genome-gene-14.244/maker-Scaffold05-snap-gene-14.59	"Protein of unknown function"/"Protein of unknown function"/"Protein of unknown function"

Scaffold05_1571204	bioclim_12	0,892504127	maker-Scaffold05-snap-gene-15.72/maker-Scaffold05-snap-gene-15.72	"Similar to ilvD: Dihydroxy-acid dehydratase (Rhodopirellula baltica (strain DSM 10527 / NCIMB 13988 / SH1) OX=243090)"/"Similar to ilvD: Dihydroxy-acid dehydratase (Rhodopirellula baltica (strain DSM 10527 / NCIMB 13988 / SH1) OX=243090)"
Scaffold05_1592034	bioclim_12	0,968920595		
Scaffold05_1592940	bioclim_12	0,968920595		
Scaffold05_1594140	bioclim_12	0,883816801	maker-Scaffold05-exonerate_est2genome-gene-16.0/"Ankyrin repeat-containing domain"	"Similar to MGA2: Protein MGA2 (Saccharomyces cerevisiae (strain ATCC 204508 / S288c) OX=559292)"/"Similar to MGA2: Protein MGA2 (Saccharomyces cerevisiae (strain ATCC 204508 / S288c) OX=559292)"
Scaffold05_1594331	bioclim_12	0,968920595	maker-Scaffold05-exonerate_est2genome-gene-16.0/"Ankyrin repeat-containing domain"	"Similar to MGA2: Protein MGA2 (Saccharomyces cerevisiae (strain ATCC 204508 / S288c) OX=559292)"/"Similar to MGA2: Protein MGA2 (Saccharomyces cerevisiae (strain ATCC 204508 / S288c) OX=559292)"
Scaffold05_1596290	bioclim_12	0,883816801	maker-Scaffold05-exonerate_est2genome-gene-16.0/"Ankyrin repeat-containing domain"	"Similar to MGA2: Protein MGA2 (Saccharomyces cerevisiae (strain ATCC 204508 / S288c) OX=559292)"/"Similar to MGA2: Protein MGA2 (Saccharomyces cerevisiae (strain ATCC 204508 / S288c) OX=559292)"
Scaffold05_1605556	bioclim_12	0,892504127	maker-Scaffold05-augustus-gene-16.52/maker-Scaffold05-augustus-gene-16.52	"Similar to Nup358: E3 SUMO-protein ligase RanBP2 (Drosophila melanogaster OX=7227)"/"Similar to Nup358: E3 SUMO-protein ligase RanBP2 (Drosophila melanogaster OX=7227)"
Scaffold05_1607515	bioclim_12	0,892504127	maker-Scaffold05-augustus-gene-16.52/maker-Scaffold05-augustus-gene-16.52	"Similar to Nup358: E3 SUMO-protein ligase RanBP2 (Drosophila melanogaster OX=7227)"/"Similar to Nup358: E3 SUMO-protein ligase RanBP2 (Drosophila melanogaster OX=7227)"
Scaffold05_1936906	bioclim_12	0,892504127	maker-Scaffold05-snap-gene-19.22/maker-Scaffold05-snap-gene-19.22	"Similar to SC3: Fruiting body protein SC3 (Schizophyllum commune OX=5334)"/"Similar to SC3: Fruiting body protein SC3 (Schizophyllum commune OX=5334)"

Scaffold05_1938007	bioclim_12	0,892504127	maker-Scaffold05-augustus-gene-19.14/maker-Scaffold05-augustus-gene-19.14	"Similar to SPBC215.06c: UPF0743 protein C215.06c (Schizosaccharomyces pombe (strain 972 / ATCC 24843) OX=284812)"/"Similar to SPBC215.06c: UPF0743 protein C215.06c (Schizosaccharomyces pombe (strain 972 / ATCC 24843) OX=284812)"
Scaffold05_4100425	bioclim_12	0,86923549	maker-Scaffold05-exonerate_est2genome-gene-41.217/maker-Scaffold05-exonerate_est2genome-gene-41.217	"Similar to Manganese peroxidase H4 (Phanerochaete chrysosporium OX=5306)"/"Similar to Manganese peroxidase H4 (Phanerochaete chrysosporium OX=5306)"
Scaffold05_4308750	bioclim_12	0,883816801		
Scaffold05_4308875	bioclim_12	0,968920595		
Scaffold05_4309400	bioclim_12	0,883816801	maker-Scaffold05-augustus-gene-43.80/maker-Scaffold05-augustus-gene-43.80	"Protein of unknown function"/"Protein of unknown function"
Scaffold05_4312091	bioclim_12	0,968920595	maker-Scaffold05-augustus-gene-43.80/maker-Scaffold05-augustus-gene-43.80	"Protein of unknown function"/"Protein of unknown function"
Scaffold05_4312142	bioclim_12	0,968920595	maker-Scaffold05-augustus-gene-43.80/maker-Scaffold05-augustus-gene-43.80	"Protein of unknown function"/"Protein of unknown function"
Scaffold05_4324939	bioclim_12	0,828248267	maker-Scaffold05-snap-gene-43.35/maker-Scaffold05-snap-gene-43.35	"Protein of unknown function"/"Protein of unknown function"

Scaffold05_4328708	bioclim_12	0,906371134	maker-Scaffold05-snap-gene-43.6/maker-Scaffold05-snap-gene-43.6	"Similar to SPBC15C4.04c: Uncharacterized amino-acid permease C15C4.04c (Schizosaccharomyces pombe (strain 972 / ATCC 24843) OX=284812)"/"Similar to SPBC15C4.04c: Uncharacterized amino-acid permease C15C4.04c (Schizosaccharomyces pombe (strain 972 / ATCC 24843) OX=284812)"
Scaffold05_4328946	bioclim_12	0,968920595	maker-Scaffold05-snap-gene-43.6/maker-Scaffold05-snap-gene-43.6	"Similar to SPBC15C4.04c: Uncharacterized amino-acid permease C15C4.04c (Schizosaccharomyces pombe (strain 972 / ATCC 24843) OX=284812)"/"Similar to SPBC15C4.04c: Uncharacterized amino-acid permease C15C4.04c (Schizosaccharomyces pombe (strain 972 / ATCC 24843) OX=284812)"
Scaffold05_4430717	bioclim_12	0,88060645	maker-Scaffold05-augustus-gene-44.84/maker-Scaffold05-augustus-gene-44.84	"Protein of unknown function"/"Protein of unknown function"
Scaffold05_4431092	bioclim_12	0,88060645		
Scaffold05_4432044	bioclim_12	0,88060645	maker-Scaffold05-augustus-gene-44.73/maker-Scaffold05-augustus-gene-44.73	"Similar to abc4: ATP-binding cassette transporter abc4 (Schizosaccharomyces pombe (strain 972 / ATCC 24843) OX=284812)"/"Similar to abc4: ATP-binding cassette transporter abc4 (Schizosaccharomyces pombe (strain 972 / ATCC 24843) OX=284812)"
Scaffold05_4432351	biocklim_3	0,842877862	maker-Scaffold05-augustus-gene-44.73/maker-Scaffold05-augustus-gene-44.73	"Similar to abc4: ATP-binding cassette transporter abc4 (Schizosaccharomyces pombe (strain 972 / ATCC 24843) OX=284812)"/"Similar to abc4: ATP-binding cassette transporter abc4 (Schizosaccharomyces pombe (strain 972 / ATCC 24843) OX=284812)"
Scaffold05_4432471	biocklim_3	0,842877862	maker-Scaffold05-augustus-gene-44.73/maker-	"Similar to abc4: ATP-binding cassette transporter abc4 (Schizosaccharomyces pombe (strain 972 / ATCC 24843) OX=284812)"/"Similar to abc4: ATP-binding cassette transporter

			Scaffold05-augustus-gene-44.73	abc4 (Schizosaccharomyces pombe (strain 972 / ATCC 24843) OX=284812)"
Scaffold05_4436050	bioclim_12	0,828248267	maker-Scaffold05-augustus-gene-44.73/maker-Scaffold05-augustus-gene-44.73	"Similar to abc4: ATP-binding cassette transporter abc4 (Schizosaccharomyces pombe (strain 972 / ATCC 24843) OX=284812)"/"Similar to abc4: ATP-binding cassette transporter abc4 (Schizosaccharomyces pombe (strain 972 / ATCC 24843) OX=284812)"
Scaffold05_4529577	bioclim_12	0,892504127	snap_masked-Scaffold05-processed-gene-45.38/snap_masked-Scaffold05-processed-gene-45.38	
Scaffold05_4877323	bioclim_12	0,892504127	maker-Scaffold05-exonerate_est2genome-gene-48.142/maker-Scaffold05-exonerate_est2genome-gene-48.142	"Protein of unknown function"/"Protein of unknown function"
Scaffold05_4924906	bioclim_12	0,892504127	maker-Scaffold05-snap-gene-49.62/maker-Scaffold05-snap-gene-49.62	
Scaffold05_4989677	bioclim_12	0,892504127		
Scaffold05_4999635	bioclim_12	0,892504127	maker-Scaffold05-snap-gene-50.1/maker-Scaffold05-snap-gene-50.1	"Similar to ENDO4: Endonuclease 4 (Arabidopsis thaliana OX=3702)"/"Similar to ENDO4: Endonuclease 4 (Arabidopsis thaliana OX=3702)"
Scaffold05_5000952	bioclim_12	0,892504127	maker-Scaffold05-snap-gene-50.1/maker-Scaffold05-snap-gene-50.1	"Similar to ENDO4: Endonuclease 4 (Arabidopsis thaliana OX=3702)"/"Similar to ENDO4: Endonuclease 4 (Arabidopsis thaliana OX=3702)"
Scaffold05_5014004	bioclim_12	0,892504127		

Scaffold05_5014812	bioclim_12	0,892504127	genemark-Scaffold05-processed-gene-50.7/genemark-Scaffold05-processed-gene-50.7	"Similar to ZRT1: Zinc-regulated transporter 1 (Saccharomyces cerevisiae (strain ATCC 204508 / S288c) OX=559292)"/"Similar to ZRT1: Zinc-regulated transporter 1 (Saccharomyces cerevisiae (strain ATCC 204508 / S288c) OX=559292)"
Scaffold05_5020019	bioclim_12	0,892504127	snap_masked-Scaffold05-processed-gene-50.34/snap_masked-Scaffold05-processed-gene-50.34	"Similar to cpaT: MFS transporter cpaT (Aspergillus oryzae OX=5062)"/"Similar to cpaT: MFS transporter cpaT (Aspergillus oryzae OX=5062)"
Scaffold05_5100518	bioclim_12	0,968920595	maker-Scaffold05-exonerate_est2genome-gene-51.0/maker-Scaffold05-exonerate_est2genome-gene-51.0	"Similar to aml: Alpha-amylase (Streptomyces violaceus OX=1936)"/"Similar to aml: Alpha-amylase (Streptomyces violaceus OX=1936)"
Scaffold05_5100609	bioclim_12	0,968920595	maker-Scaffold05-exonerate_est2genome-gene-51.0/maker-Scaffold05-exonerate_est2genome-gene-51.0	"Similar to aml: Alpha-amylase (Streptomyces violaceus OX=1936)"/"Similar to aml: Alpha-amylase (Streptomyces violaceus OX=1936)"
Scaffold05_5100795	bioclim_12	0,892504127	maker-Scaffold05-exonerate_est2genome-gene-51.0/maker-Scaffold05-exonerate_est2genome-gene-51.0	"Similar to aml: Alpha-amylase (Streptomyces violaceus OX=1936)"/"Similar to aml: Alpha-amylase (Streptomyces violaceus OX=1936)"
Scaffold05_5102422	bioclim_12	0,968920595	maker-Scaffold05-exonerate_est2genome-gene-51.0/maker-	"Similar to aml: Alpha-amylase (Streptomyces violaceus OX=1936)"/"Similar to aml: Alpha-amylase (Streptomyces violaceus OX=1936)"

			Scaffold05-exonerate_est2genome-gene-51.0	
Scaffold05_5102452	bioclim_12	0,968920595	maker-Scaffold05-exonerate_est2genome-gene-51.0/maker-Scaffold05-exonerate_est2genome-gene-51.0	"Similar to aml: Alpha-amylase (Streptomyces violaceus OX=1936)"/"Similar to aml: Alpha-amylase (Streptomyces violaceus OX=1936)"
Scaffold05_5102703	bioclim_12	0,968920595	maker-Scaffold05-exonerate_est2genome-gene-51.0/maker-Scaffold05-exonerate_est2genome-gene-51.0	"Similar to aml: Alpha-amylase (Streptomyces violaceus OX=1936)"/"Similar to aml: Alpha-amylase (Streptomyces violaceus OX=1936)"
Scaffold05_5102784	bioclim_12	0,968920595	maker-Scaffold05-exonerate_est2genome-gene-51.0/maker-Scaffold05-exonerate_est2genome-gene-51.0	"Similar to aml: Alpha-amylase (Streptomyces violaceus OX=1936)"/"Similar to aml: Alpha-amylase (Streptomyces violaceus OX=1936)"
Scaffold05_5102808	bioclim_12	0,968920595	maker-Scaffold05-exonerate_est2genome-gene-51.0/maker-Scaffold05-exonerate_est2genome-gene-51.0	"Similar to aml: Alpha-amylase (Streptomyces violaceus OX=1936)"/"Similar to aml: Alpha-amylase (Streptomyces violaceus OX=1936)"
Scaffold05_5103466	bioclim_12	0,968920595	maker-Scaffold05-exonerate_est2genome-gene-51.0/maker-	"Similar to aml: Alpha-amylase (Streptomyces violaceus OX=1936)"/"Similar to aml: Alpha-amylase (Streptomyces violaceus OX=1936)"

			Scaffold05-exonerate_est2genome-gene-51.0	
Scaffold05_5103637	bioclim_12	0,968920595	maker-Scaffold05-exonerate_est2genome-gene-51.0/maker-Scaffold05-exonerate_est2genome-gene-51.0	"Similar to aml: Alpha-amylase (Streptomyces violaceus OX=1936)"/"Similar to aml: Alpha-amylase (Streptomyces violaceus OX=1936)"
Scaffold05_5104892	bioclim_12	0,968920595	maker-Scaffold05-snap-gene-51.57/maker-Scaffold05-snap-gene-51.57	"Similar to sirN: N-methyltransferase sirN (Leptosphaeria maculans OX=5022)"/"Similar to sirN: N-methyltransferase sirN (Leptosphaeria maculans OX=5022)"
Scaffold05_5105966	bioclim_12	0,968920595		
Scaffold05_5107148	bioclim_12	0,892504127	genemark-Scaffold05-processed-gene-51.4/genemark-Scaffold05-processed-gene-51.4	"Similar to easB: Highly reducing polyketide synthase easB (Emericella nidulans (strain FGSC A4 / ATCC 38163 / CBS 112.46 / NRRL 194 / M139) OX=227321)"
Scaffold05_5110717	bioclim_12	0,968920595	genemark-Scaffold05-processed-gene-51.4/genemark-Scaffold05-processed-gene-51.4	"Similar to easB: Highly reducing polyketide synthase easB (Emericella nidulans (strain FGSC A4 / ATCC 38163 / CBS 112.46 / NRRL 194 / M139) OX=227321)"
Scaffold05_5111663	bioclim_12	0,968920595	genemark-Scaffold05-processed-gene-51.4/genemark-Scaffold05-processed-gene-51.4	"Similar to easB: Highly reducing polyketide synthase easB (Emericella nidulans (strain FGSC A4 / ATCC 38163 / CBS 112.46 / NRRL 194 / M139) OX=227321)"
Scaffold05_5111809	bioclim_12	0,968920595	genemark-Scaffold05-processed-gene-51.4/genemark-Scaffold05-processed-gene-51.4	"Similar to easB: Highly reducing polyketide synthase easB (Emericella nidulans (strain FGSC A4 / ATCC 38163 / CBS 112.46 / NRRL 194 / M139) OX=227321)"

Scaffold05_5111923	bioclim_12	0,913883477	genemark-Scaffold05-processed-gene-51.4/genemark-Scaffold05-processed-gene-51.4	"Similar to easB: Highly reducing polyketide synthase easB (Emericella nidulans (strain FGSC A4 / ATCC 38163 / CBS 112.46 / NRRL 194 / M139) OX=227321)"
Scaffold05_5111956	bioclim_12	0,913883477	genemark-Scaffold05-processed-gene-51.4/genemark-Scaffold05-processed-gene-51.4	"Similar to easB: Highly reducing polyketide synthase easB (Emericella nidulans (strain FGSC A4 / ATCC 38163 / CBS 112.46 / NRRL 194 / M139) OX=227321)"
Scaffold05_5112180	bioclim_12	0,892504127	genemark-Scaffold05-processed-gene-51.4/genemark-Scaffold05-processed-gene-51.4	"Similar to easB: Highly reducing polyketide synthase easB (Emericella nidulans (strain FGSC A4 / ATCC 38163 / CBS 112.46 / NRRL 194 / M139) OX=227321)"
Scaffold05_5122094	bioclim_12	0,892504127	maker-Scaffold05-snap-gene-51.4/maker-Scaffold05-snap-gene-51.4	"Similar to yakc: Aldo-keto reductase yakc [NADP(+)] (Schizosaccharomyces pombe (strain 972 / ATCC 24843) OX=284812)"/"Similar to yakc: Aldo-keto reductase yakc [NADP(+)] (Schizosaccharomyces pombe (strain 972 / ATCC 24843) OX=284812)"
Scaffold05_5122281	bioclim_12	0,892504127	maker-Scaffold05-snap-gene-51.4/maker-Scaffold05-snap-gene-51.4	"Similar to yakc: Aldo-keto reductase yakc [NADP(+)] (Schizosaccharomyces pombe (strain 972 / ATCC 24843) OX=284812)"/"Similar to yakc: Aldo-keto reductase yakc [NADP(+)] (Schizosaccharomyces pombe (strain 972 / ATCC 24843) OX=284812)"
Scaffold05_5131664	bioclim_12	0,892504127		
Scaffold05_5567906	bioclim_12	0,828248267	maker-Scaffold05-snap-gene-55.67/maker-Scaffold05-snap-gene-55.67	"Similar to rqh1: ATP-dependent DNA helicase hus2/rqh1 (Schizosaccharomyces pombe (strain 972 / ATCC 24843) OX=284812)"/"Similar to rqh1: ATP-dependent DNA helicase hus2/rqh1 (Schizosaccharomyces pombe (strain 972 / ATCC 24843) OX=284812)"

Scaffold05_5568237	bioclim_12	0,906371134	maker-Scaffold05-snap-gene-55.67/maker-Scaffold05-snap-gene-55.67	"Similar to rqh1: ATP-dependent DNA helicase hus2/rqh1 (Schizosaccharomyces pombe (strain 972 / ATCC 24843) OX=284812)"/"Similar to rqh1: ATP-dependent DNA helicase hus2/rqh1 (Schizosaccharomyces pombe (strain 972 / ATCC 24843) OX=284812)"
Scaffold05_5617010	bioclim_12	0,906371134	maker-Scaffold05-snap-gene-56.30/maker-Scaffold05-snap-gene-56.30	"Similar to Arp1: Scytalone dehydratase-like protein Arp1 (Metarhizium brunneum (strain ARSEF 3297) OX=1276141)"/"Similar to Arp1: Scytalone dehydratase-like protein Arp1 (Metarhizium brunneum (strain ARSEF 3297) OX=1276141)"
Scaffold05_5617016	bioclim_12	0,906371134	maker-Scaffold05-snap-gene-56.30/maker-Scaffold05-snap-gene-56.30	"Similar to Arp1: Scytalone dehydratase-like protein Arp1 (Metarhizium brunneum (strain ARSEF 3297) OX=1276141)"/"Similar to Arp1: Scytalone dehydratase-like protein Arp1 (Metarhizium brunneum (strain ARSEF 3297) OX=1276141)"
Scaffold05_5618125	bioclim_12	0,968920595	maker-Scaffold05-snap-gene-56.30/maker-Scaffold05-snap-gene-56.30	"Similar to Arp1: Scytalone dehydratase-like protein Arp1 (Metarhizium brunneum (strain ARSEF 3297) OX=1276141)"/"Similar to Arp1: Scytalone dehydratase-like protein Arp1 (Metarhizium brunneum (strain ARSEF 3297) OX=1276141)"
Scaffold05_5618221	bioclim_12	0,88060645	maker-Scaffold05-snap-gene-56.30/maker-Scaffold05-snap-gene-56.30	"Similar to Arp1: Scytalone dehydratase-like protein Arp1 (Metarhizium brunneum (strain ARSEF 3297) OX=1276141)"/"Similar to Arp1: Scytalone dehydratase-like protein Arp1 (Metarhizium brunneum (strain ARSEF 3297) OX=1276141)"
Scaffold05_5619175	bioclim_12	0,88060645	maker-Scaffold05-snap-gene-56.30/maker-Scaffold05-snap-gene-56.30	"Similar to Arp1: Scytalone dehydratase-like protein Arp1 (Metarhizium brunneum (strain ARSEF 3297) OX=1276141)"/"Similar to Arp1: Scytalone dehydratase-like protein Arp1 (Metarhizium brunneum (strain ARSEF 3297) OX=1276141)"

Scaffold05_5620527	bioclim_12	0,968920595	maker-Scaffold05-snap-gene-56.30/maker-Scaffold05-snap-gene-56.30	"Similar to Arp1: Scytalone dehydratase-like protein Arp1 (Metarhizium brunneum (strain ARSEF 3297) OX=1276141)"/"Similar to Arp1: Scytalone dehydratase-like protein Arp1 (Metarhizium brunneum (strain ARSEF 3297) OX=1276141)"
Scaffold05_5620629	bioclim_12	0,968920595	maker-Scaffold05-snap-gene-56.30/maker-Scaffold05-snap-gene-56.30	"Similar to Arp1: Scytalone dehydratase-like protein Arp1 (Metarhizium brunneum (strain ARSEF 3297) OX=1276141)"/"Similar to Arp1: Scytalone dehydratase-like protein Arp1 (Metarhizium brunneum (strain ARSEF 3297) OX=1276141)"
Scaffold05_5622147	bioclim_12	0,968920595	snap_masked-Scaffold05-abinit-gene-56.24/snap_masked-Scaffold05-abinit-gene-56.24	"Similar to swc5: SWR1-complex protein 5 (Emericella nidulans (strain FGSC A4 / ATCC 38163 / CBS 112.46 / NRRL 194 / M139) OX=227321)"/"Similar to swc5: SWR1-complex protein 5 (Emericella nidulans (strain FGSC A4 / ATCC 38163 / CBS 112.46 / NRRL 194 / M139) OX=227321)"
Scaffold05_5622282	bioclim_12	0,968920595	snap_masked-Scaffold05-abinit-gene-56.24/snap_masked-Scaffold05-abinit-gene-56.24	"Similar to swc5: SWR1-complex protein 5 (Emericella nidulans (strain FGSC A4 / ATCC 38163 / CBS 112.46 / NRRL 194 / M139) OX=227321)"/"Similar to swc5: SWR1-complex protein 5 (Emericella nidulans (strain FGSC A4 / ATCC 38163 / CBS 112.46 / NRRL 194 / M139) OX=227321)"
Scaffold05_5622477	bioclim_12	0,968920595	snap_masked-Scaffold05-abinit-gene-56.24/snap_masked-Scaffold05-abinit-gene-56.24	"Similar to swc5: SWR1-complex protein 5 (Emericella nidulans (strain FGSC A4 / ATCC 38163 / CBS 112.46 / NRRL 194 / M139) OX=227321)"/"Similar to swc5: SWR1-complex protein 5 (Emericella nidulans (strain FGSC A4 / ATCC 38163 / CBS 112.46 / NRRL 194 / M139) OX=227321)"
Scaffold05_5623806	bioclim_12	0,806497657	genemark-Scaffold05-processed-gene-56.8/genemark-Scaffold05-processed-gene-56.8	"Protein of unknown function"/"Protein of unknown function"

Scaffold05_5624462	bioclim_12	0,968920595	genemark-Scaffold05-processed-gene-56.8/genemark-Scaffold05-processed-gene-56.8	"Protein of unknown function"/"Protein of unknown function"
Scaffold05_5625600	bioclim_12	0,968920595	genemark-Scaffold05-processed-gene-56.8/genemark-Scaffold05-processed-gene-56.8	"Protein of unknown function"/"Protein of unknown function"
Scaffold05_5627634	bioclim_12	0,968920595	maker-Scaffold05-snap-gene-56.4/maker-Scaffold05-snap-gene-56.4	"Protein of unknown function"/"Protein of unknown function"
Scaffold05_5628326	bioclim_12	0,968920595	maker-Scaffold05-snap-gene-56.4/maker-Scaffold05-snap-gene-56.4	"Protein of unknown function"/"Protein of unknown function"
Scaffold05_5632269	bioclim_12	0,968920595		
Scaffold05_5668503	bioclim_12	0,913883477	maker-Scaffold05-snap-gene-56.34/maker-Scaffold05-snap-gene-56.47/maker-Scaffold05-snap-gene-56.34	"Similar to SPBC2A9.02: Uncharacterized protein C2A9.02 (Schizosaccharomyces pombe (strain 972 / ATCC 24843) OX=284812)"/"Similar to SPAC824.03c: Uncharacterized protein C824.03c, mitochondrial (Schizosaccharomyces pombe (strain 972 / ATCC 24843) OX=284812)"
Scaffold05_5668527	bioclim_12	0,913883477	maker-Scaffold05-snap-gene-56.34/maker-Scaffold05-snap-gene-56.47/maker-Scaffold05-snap-gene-56.34	"Similar to SPBC2A9.02: Uncharacterized protein C2A9.02 (Schizosaccharomyces pombe (strain 972 / ATCC 24843) OX=284812)"/"Similar to SPAC824.03c: Uncharacterized protein C824.03c, mitochondrial (Schizosaccharomyces pombe (strain 972 / ATCC 24843) OX=284812)"
Scaffold05_5668671	bioclim_12	0,968920595	maker-Scaffold05-snap-gene-56.34/maker-Scaffold05-snap-gene-56.47/maker-Scaffold05-snap-gene-56.34	"Similar to SPBC2A9.02: Uncharacterized protein C2A9.02 (Schizosaccharomyces pombe (strain 972 / ATCC 24843) OX=284812)"/"Similar to SPAC824.03c: Uncharacterized protein C824.03c, mitochondrial (Schizosaccharomyces pombe (strain 972 / ATCC 24843) OX=284812)"

Scaffold05_5672411	bioclim_12	0,806497657	maker-Scaffold05-augustus-gene-56.30/maker-Scaffold05-augustus-gene-56.30	"Protein of unknown function"/"Protein of unknown function"
Scaffold05_5673085	bioclim_12	0,968920595	maker-Scaffold05-augustus-gene-56.30/maker-Scaffold05-augustus-gene-56.30	"Protein of unknown function"/"Protein of unknown function"
Scaffold05_5674022	bioclim_12	0,968920595	maker-Scaffold05-augustus-gene-56.30/maker-Scaffold05-augustus-gene-56.30	"Protein of unknown function"/"Protein of unknown function"
Scaffold05_5674538	bioclim_12	0,968920595	maker-Scaffold05-augustus-gene-56.30/maker-Scaffold05-augustus-gene-56.30	"Protein of unknown function"/"Protein of unknown function"
Scaffold05_5675937	bioclim_12	0,968920595		
Scaffold05_5680254	bioclim_12	0,968920595	snap_masked-Scaffold05-processed-gene-56.49/snap_masked-Scaffold05-processed-gene-56.49	"Similar to GPA4: Guanine nucleotide-binding protein alpha-4 subunit (Ustilago maydis (strain 521 / FGSC 9021) OX=237631)"/"Similar to GPA4: Guanine nucleotide-binding protein alpha-4 subunit (Ustilago maydis (strain 521 / FGSC 9021) OX=237631)"
Scaffold05_5680758	bioclim_12	0,968920595	snap_masked-Scaffold05-processed-gene-56.49/snap_masked-Scaffold05-processed-gene-56.49	"Similar to GPA4: Guanine nucleotide-binding protein alpha-4 subunit (Ustilago maydis (strain 521 / FGSC 9021) OX=237631)"/"Similar to GPA4: Guanine nucleotide-binding protein alpha-4 subunit (Ustilago maydis (strain 521 / FGSC 9021) OX=237631)"
Scaffold05_5680957	bioclim_12	0,968920595	snap_masked-Scaffold05-processed-gene-56.49/snap_masked-	"Similar to GPA4: Guanine nucleotide-binding protein alpha-4 subunit (Ustilago maydis (strain 521 / FGSC 9021) OX=237631)"/"Similar to GPA4: Guanine nucleotide-binding

			Scaffold05-processed-gene-56.49	protein alpha-4 subunit (Ustilago maydis (strain 521 / FGSC 9021) OX=237631)"
Scaffold05_5685704	bioclim_12	0,968920595	maker-Scaffold05-snap-gene-56.49/maker-Scaffold05-snap-gene-56.49	"Protein of unknown function"/"Protein of unknown function"
Scaffold05_5685712	bioclim_12	0,968920595	maker-Scaffold05-snap-gene-56.49/maker-Scaffold05-snap-gene-56.49	"Protein of unknown function"/"Protein of unknown function"
Scaffold05_5686122	bioclim_12	0,968920595	maker-Scaffold05-snap-gene-56.49/maker-Scaffold05-snap-gene-56.49	"Protein of unknown function"/"Protein of unknown function"
Scaffold05_5690854	bioclim_12	0,968920595	snap_masked-Scaffold05-processed-gene-57.12/snap_masked-Scaffold05-processed-gene-57.12	"Protein of unknown function"/"Protein of unknown function"
Scaffold05_5692706	bioclim_12	0,968920595	snap_masked-Scaffold05-abinit-gene-57.2/snap_masked-Scaffold05-abinit-gene-57.2	"Similar to SP2: Subtilisin-like protease 2 (Pseudogymnoascus destructans (strain ATCC MYA-4855 / 20631-21) OX=658429)"/"Similar to SP2: Subtilisin-like protease 2 (Pseudogymnoascus destructans (strain ATCC MYA-4855 / 20631-21) OX=658429)"
Scaffold05_5693569	bioclim_12	0,968920595	snap_masked-Scaffold05-abinit-gene-57.2/snap_masked-Scaffold05-abinit-gene-57.2	"Similar to SP2: Subtilisin-like protease 2 (Pseudogymnoascus destructans (strain ATCC MYA-4855 / 20631-21) OX=658429)"/"Similar to SP2: Subtilisin-like protease 2 (Pseudogymnoascus destructans (strain ATCC MYA-4855 / 20631-21) OX=658429)"
Scaffold05_5693837	bioclim_12	0,968920595	snap_masked-Scaffold05-abinit-gene-57.2/snap_masked-Scaffold05-abinit-gene-57.2	"Similar to SP2: Subtilisin-like protease 2 (Pseudogymnoascus destructans (strain ATCC MYA-4855 / 20631-21) OX=658429)"/"Similar to SP2: Subtilisin-like protease 2

				(Pseudogymnoascus destructans (strain ATCC MYA-4855 / 20631-21) OX=658429)"
Scaffold05_5694630	bioclim_12	0,968920595	snap_masked-Scaffold05-abinit-gene-57.2/snap_masked-Scaffold05-abinit-gene-57.2	"Similar to SP2: Subtilisin-like protease 2 (Pseudogymnoascus destructans (strain ATCC MYA-4855 / 20631-21) OX=658429)"/"Similar to SP2: Subtilisin-like protease 2 (Pseudogymnoascus destructans (strain ATCC MYA-4855 / 20631-21) OX=658429)"
Scaffold05_5695090	bioclim_12	0,968920595	snap_masked-Scaffold05-abinit-gene-57.2/snap_masked-Scaffold05-abinit-gene-57.2	"Similar to SP2: Subtilisin-like protease 2 (Pseudogymnoascus destructans (strain ATCC MYA-4855 / 20631-21) OX=658429)"/"Similar to SP2: Subtilisin-like protease 2 (Pseudogymnoascus destructans (strain ATCC MYA-4855 / 20631-21) OX=658429)"
Scaffold05_5695170	bioclim_12	0,968920595	snap_masked-Scaffold05-abinit-gene-57.2/snap_masked-Scaffold05-abinit-gene-57.2	"Similar to SP2: Subtilisin-like protease 2 (Pseudogymnoascus destructans (strain ATCC MYA-4855 / 20631-21) OX=658429)"/"Similar to SP2: Subtilisin-like protease 2 (Pseudogymnoascus destructans (strain ATCC MYA-4855 / 20631-21) OX=658429)"
Scaffold05_5695187	bioclim_12	0,968920595	snap_masked-Scaffold05-abinit-gene-57.2/snap_masked-Scaffold05-abinit-gene-57.2	"Similar to SP2: Subtilisin-like protease 2 (Pseudogymnoascus destructans (strain ATCC MYA-4855 / 20631-21) OX=658429)"/"Similar to SP2: Subtilisin-like protease 2 (Pseudogymnoascus destructans (strain ATCC MYA-4855 / 20631-21) OX=658429)"
Scaffold05_5695371	bioclim_12	0,968920595	snap_masked-Scaffold05-abinit-gene-57.2/snap_masked-Scaffold05-abinit-gene-57.2	"Similar to SP2: Subtilisin-like protease 2 (Pseudogymnoascus destructans (strain ATCC MYA-4855 / 20631-21) OX=658429)"/"Similar to SP2: Subtilisin-like protease 2 (Pseudogymnoascus destructans (strain ATCC MYA-4855 / 20631-21) OX=658429)"
Scaffold05_5696763	bioclim_12	0,968920595	maker-Scaffold05-snap-gene-57.17/maker-Scaffold05-snap-gene-57.17	"Similar to SLN1: Osmosensing histidine protein kinase SLN1 (Saccharomyces cerevisiae (strain ATCC 204508 / S288c) OX=559292)"/"Similar to SLN1: Osmosensing histidine protein

				kinase SLN1 (Saccharomyces cerevisiae (strain ATCC 204508 / S288c) OX=559292)"
Scaffold05_5696818	bioclim_12	0,968920595	maker-Scaffold05-snap-gene-57.17/maker-Scaffold05-snap-gene-57.17	"Similar to SLN1: Osmosensing histidine protein kinase SLN1 (Saccharomyces cerevisiae (strain ATCC 204508 / S288c) OX=559292)"/"Similar to SLN1: Osmosensing histidine protein kinase SLN1 (Saccharomyces cerevisiae (strain ATCC 204508 / S288c) OX=559292)"
Scaffold05_5696990	bioclim_12	0,968920595	maker-Scaffold05-snap-gene-57.17/maker-Scaffold05-snap-gene-57.17	"Similar to SLN1: Osmosensing histidine protein kinase SLN1 (Saccharomyces cerevisiae (strain ATCC 204508 / S288c) OX=559292)"/"Similar to SLN1: Osmosensing histidine protein kinase SLN1 (Saccharomyces cerevisiae (strain ATCC 204508 / S288c) OX=559292)"
Scaffold05_5698323	bioclim_12	0,968920595	maker-Scaffold05-snap-gene-57.17/maker-Scaffold05-snap-gene-57.17	"Similar to SLN1: Osmosensing histidine protein kinase SLN1 (Saccharomyces cerevisiae (strain ATCC 204508 / S288c) OX=559292)"/"Similar to SLN1: Osmosensing histidine protein kinase SLN1 (Saccharomyces cerevisiae (strain ATCC 204508 / S288c) OX=559292)"
Scaffold05_5698379	bioclim_12	0,968920595	maker-Scaffold05-snap-gene-57.17/maker-Scaffold05-snap-gene-57.17	"Similar to SLN1: Osmosensing histidine protein kinase SLN1 (Saccharomyces cerevisiae (strain ATCC 204508 / S288c) OX=559292)"/"Similar to SLN1: Osmosensing histidine protein kinase SLN1 (Saccharomyces cerevisiae (strain ATCC 204508 / S288c) OX=559292)"
Scaffold05_5698678	bioclim_12	0,968920595	maker-Scaffold05-snap-gene-57.17/maker-Scaffold05-snap-gene-57.17	"Similar to SLN1: Osmosensing histidine protein kinase SLN1 (Saccharomyces cerevisiae (strain ATCC 204508 / S288c) OX=559292)"/"Similar to SLN1: Osmosensing histidine protein kinase SLN1 (Saccharomyces cerevisiae (strain ATCC 204508 / S288c) OX=559292)"
Scaffold05_5699785	bioclim_12	0,968920595	maker-Scaffold05-snap-gene-57.17/maker-Scaffold05-snap-gene-57.17	"Similar to SLN1: Osmosensing histidine protein kinase SLN1 (Saccharomyces cerevisiae (strain ATCC 204508 / S288c) OX=559292)"/"Similar to SLN1: Osmosensing histidine protein

				kinase SLN1 (Saccharomyces cerevisiae (strain ATCC 204508 / S288c) OX=559292)"
Scaffold05_5700031	bioclim_12	0,968920595	maker-Scaffold05-snap-gene-57.17/maker-Scaffold05-snap-gene-57.17	"Similar to SLN1: Osmosensing histidine protein kinase SLN1 (Saccharomyces cerevisiae (strain ATCC 204508 / S288c) OX=559292)"/"Similar to SLN1: Osmosensing histidine protein kinase SLN1 (Saccharomyces cerevisiae (strain ATCC 204508 / S288c) OX=559292)"
Scaffold05_5700528	bioclim_12	0,968920595	maker-Scaffold05-snap-gene-57.17/maker-Scaffold05-snap-gene-57.17	"Similar to SLN1: Osmosensing histidine protein kinase SLN1 (Saccharomyces cerevisiae (strain ATCC 204508 / S288c) OX=559292)"/"Similar to SLN1: Osmosensing histidine protein kinase SLN1 (Saccharomyces cerevisiae (strain ATCC 204508 / S288c) OX=559292)"
Scaffold05_5702874	bioclim_12	0,835492909	maker-Scaffold05-snap-gene-57.59/maker-Scaffold05-snap-gene-57.59	
Scaffold05_5703480	bioclim_12	0,968920595	maker-Scaffold05-snap-gene-57.59/maker-Scaffold05-snap-gene-57.59	"Similar to lysA: Saccharopine dehydrogenase [NAD(+), L-lysine-forming] (Emericella nidulans (strain FGSC A4 / ATCC 38163 / CBS 112.46 / NRRL 194 / M139) OX=227321)"
Scaffold05_5704177	bioclim_12	0,835492909	maker-Scaffold05-snap-gene-57.59/maker-Scaffold05-snap-gene-57.59	"Similar to lysA: Saccharopine dehydrogenase [NAD(+), L-lysine-forming] (Emericella nidulans (strain FGSC A4 / ATCC 38163 / CBS 112.46 / NRRL 194 / M139) OX=227321)"
Scaffold05_5704851	bioclim_12	0,968920595	snap_masked-Scaffold05-processed-gene-57.15/snap_masked-Scaffold05-processed-gene-57.15	"Similar to lysA: Saccharopine dehydrogenase [NAD(+), L-lysine-forming] (Emericella nidulans (strain FGSC A4 / ATCC 38163 / CBS 112.46 / NRRL 194 / M139) OX=227321)"
Scaffold05_5704880	bioclim_12	0,968920595	snap_masked-Scaffold05-processed-gene-57.15/snap_masked-	"Similar to arg-13: Amino-acid transporter arg-13 (Neurospora crassa (strain ATCC 24698 / 74-OR23-1A / CBS 708.71 / DSM 1257 / FGSC 987) OX=367110)"/"Similar to arg-13: Amino-acid

			Scaffold05-processed-gene-57.15	transporter arg-13 (Neurospora crassa (strain ATCC 24698 / 74-OR23-1A / CBS 708.71 / DSM 1257 / FGSC 987) OX=367110)"
Scaffold05_5707341	bioclim_12	0,968920595	maker-Scaffold05-augustus-gene-57.23/maker-Scaffold05-augustus-gene-57.23	"Protein of unknown function"/"Protein of unknown function"
Scaffold05_5710401	bioclim_12	0,968920595	maker-Scaffold05-augustus-gene-57.23/maker-Scaffold05-snap-gene-57.60/maker-Scaffold05-augustus-gene-57.23	"Protein of unknown function"/"Similar to arg-13: Amino-acid transporter arg-13 (Neurospora crassa (strain ATCC 24698 / 74-OR23-1A / CBS 708.71 / DSM 1257 / FGSC 987) OX=367110)"/"Protein of unknown function"
Scaffold05_5710674	bioclim_12	0,867584111	maker-Scaffold05-augustus-gene-57.23/maker-Scaffold05-snap-gene-57.60/maker-Scaffold05-augustus-gene-57.23	"Protein of unknown function"/"Similar to arg-13: Amino-acid transporter arg-13 (Neurospora crassa (strain ATCC 24698 / 74-OR23-1A / CBS 708.71 / DSM 1257 / FGSC 987) OX=367110)"/"Protein of unknown function"
Scaffold05_5711714	bioclim_12	0,923108221	maker-Scaffold05-snap-gene-57.60/maker-Scaffold05-snap-gene-57.60	"Similar to arg-13: Amino-acid transporter arg-13 (Neurospora crassa (strain ATCC 24698 / 74-OR23-1A / CBS 708.71 / DSM 1257 / FGSC 987) OX=367110)"/"Similar to arg-13: Amino-acid transporter arg-13 (Neurospora crassa (strain ATCC 24698 / 74-OR23-1A / CBS 708.71 / DSM 1257 / FGSC 987) OX=367110)"
Scaffold05_5713553	bioclim_12	0,968920595	maker-Scaffold05-augustus-gene-57.24/maker-Scaffold05-augustus-gene-57.24	"Similar to YBR139W: Putative serine carboxypeptidase YBR139W (Saccharomyces cerevisiae (strain ATCC 204508 / S288c) OX=559292)"/"Similar to YBR139W: Putative serine carboxypeptidase YBR139W (Saccharomyces cerevisiae (strain ATCC 204508 / S288c) OX=559292)"
Scaffold05_5713894	bioclim_12	0,968920595	maker-Scaffold05-augustus-gene-57.24/maker-Scaffold05-augustus-gene-57.24	"Similar to YBR139W: Putative serine carboxypeptidase YBR139W (Saccharomyces cerevisiae (strain ATCC 204508 / S288c) OX=559292)"/"Similar to YBR139W: Putative serine

				carboxypeptidase YBR139W (Saccharomyces cerevisiae (strain ATCC 204508 / S288c) OX=559292)"
Scaffold05_5714123	bioclim_12	0,968920595	maker-Scaffold05-augustus-gene-57.24/maker-Scaffold05-augustus-gene-57.24	"Similar to YBR139W: Putative serine carboxypeptidase YBR139W (Saccharomyces cerevisiae (strain ATCC 204508 / S288c) OX=559292)"/"Similar to YBR139W: Putative serine carboxypeptidase YBR139W (Saccharomyces cerevisiae (strain ATCC 204508 / S288c) OX=559292)"
Scaffold05_5715619	bioclim_12	0,968920595	maker-Scaffold05-augustus-gene-57.24/maker-Scaffold05-augustus-gene-57.24	"Similar to YBR139W: Putative serine carboxypeptidase YBR139W (Saccharomyces cerevisiae (strain ATCC 204508 / S288c) OX=559292)"/"Similar to YBR139W: Putative serine carboxypeptidase YBR139W (Saccharomyces cerevisiae (strain ATCC 204508 / S288c) OX=559292)"
Scaffold05_5715927	bioclim_12	0,968920595	maker-Scaffold05-augustus-gene-57.24/maker-Scaffold05-augustus-gene-57.24	"Similar to YBR139W: Putative serine carboxypeptidase YBR139W (Saccharomyces cerevisiae (strain ATCC 204508 / S288c) OX=559292)"/"Similar to YBR139W: Putative serine carboxypeptidase YBR139W (Saccharomyces cerevisiae (strain ATCC 204508 / S288c) OX=559292)"
Scaffold05_5716662	bioclim_12	0,968920595	maker-Scaffold05-augustus-gene-57.24/maker-Scaffold05-augustus-gene-57.24	"Similar to YBR139W: Putative serine carboxypeptidase YBR139W (Saccharomyces cerevisiae (strain ATCC 204508 / S288c) OX=559292)"/"Similar to YBR139W: Putative serine carboxypeptidase YBR139W (Saccharomyces cerevisiae (strain ATCC 204508 / S288c) OX=559292)"
Scaffold05_6270088	bioclim_12	0,906371134	maker-Scaffold05-snap-gene-62.28/maker-Scaffold05-snap-gene-62.28	"Similar to amt1: Ammonium transporter 1 (Schizosaccharomyces pombe (strain 972 / ATCC 24843) OX=284812)"/"Similar to amt1: Ammonium transporter 1 (Schizosaccharomyces pombe (strain 972 / ATCC 24843) OX=284812)"
Scaffold05_6270945	bioclim_12	0,831344217	maker-Scaffold05-snap-gene-62.28/maker-Scaffold05-snap-gene-62.28	"Similar to amt1: Ammonium transporter 1 (Schizosaccharomyces pombe (strain 972 / ATCC 24843) OX=284812)"/"Similar to amt1: Ammonium transporter 1

				(Schizosaccharomyces pombe (strain 972 / ATCC 24843) OX=284812)"
Scaffold06_681071	bioclim_12	0,906371134	maker-Scaffold06-augustus-gene-6.9/maker-Scaffold06-augustus-gene-6.9	"Similar to rgxA: Putative galacturan 1,4-alpha-galacturonidase A (Aspergillus niger OX=5061)"/"Similar to rgxA: Putative galacturan 1,4-alpha-galacturonidase A (Aspergillus niger OX=5061)"
Scaffold06_713320	bioclim_12	0,831344217	maker-Scaffold06-augustus-gene-7.6/maker-Scaffold06-augustus-gene-7.6/"Ferric reductase/ NAD binding domain"	"Similar to noxA: Superoxide-generating NADPH oxidase heavy chain subunit A (Dictyostelium discoideum OX=44689)"/"Similar to noxA: Superoxide-generating NADPH oxidase heavy chain subunit A (Dictyostelium discoideum OX=44689)"
Scaffold07_2104754	bioclim_12	0,923108221	maker-Scaffold07-augustus-gene-21.28/maker-Scaffold07-augustus-gene-21.28	
Scaffold07_2110508	bioclim_12	0,835492909	snap_masked-Scaffold07-processed-gene-21.56/snap_masked-Scaffold07-processed-gene-21.56	"Similar to SPBC530.05: Uncharacterized transcriptional regulatory protein C530.05 (Schizosaccharomyces pombe (strain 972 / ATCC 24843) OX=284812)"/"Similar to SPBC530.05: Uncharacterized transcriptional regulatory protein C530.05 (Schizosaccharomyces pombe (strain 972 / ATCC 24843) OX=284812)"
Scaffold08_1526018	bioclim_12	0,892504127	maker-Scaffold08-augustus-gene-15.77/maker-Scaffold08-augustus-gene-15.77	"Similar to Glucan 1,3-beta-glucosidase (Schwanniomyces occidentalis OX=27300)"/"Similar to Glucan 1,3-beta-glucosidase (Schwanniomyces occidentalis OX=27300)"
Scaffold08_1706943	bioclim_12	0,968920595		
Scaffold08_1706985	bioclim_12	0,968920595		
Scaffold08_1707300	bioclim_12	0,968920595		
Scaffold08_1707505	bioclim_12	0,968920595	maker-Scaffold08-exonerate_est2genome-	

			gene-17.16/maker-Scaffold08-exonerate_est2genome-gene-17.16	
Scaffold08_1707625	bioclim_12	0,968920595	maker-Scaffold08-exonerate_est2genome-gene-17.16/maker-Scaffold08-exonerate_est2genome-gene-17.16	
Scaffold08_1708230	bioclim_12	0,968920595	maker-Scaffold08-exonerate_est2genome-gene-17.16/maker-Scaffold08-exonerate_est2genome-gene-17.16	
Scaffold08_1723797	bioclim_12	0,892504127		
Scaffold08_1724086	bioclim_12	0,892504127		
Scaffold08_1726495	bioclim_12	0,923108221	maker-Scaffold08-exonerate_est2genome-gene-17.2/maker-Scaffold08-exonerate_est2genome-gene-17.2	"Similar to apdG: Acyl-CoA dehydrogenase apdG (Emericella nidulans (strain FGSC A4 / ATCC 38163 / CBS 112.46 / NRRL 194 / M139) OX=227321)"/"Similar to apdG: Acyl-CoA dehydrogenase apdG (Emericella nidulans (strain FGSC A4 / ATCC 38163 / CBS 112.46 / NRRL 194 / M139) OX=227321)"
Scaffold08_1726833	bioclim_12	0,968920595	maker-Scaffold08-exonerate_est2genome-gene-17.2/maker-Scaffold08-exonerate_est2genome-gene-17.2	"Similar to apdG: Acyl-CoA dehydrogenase apdG (Emericella nidulans (strain FGSC A4 / ATCC 38163 / CBS 112.46 / NRRL 194 / M139) OX=227321)"/"Similar to apdG: Acyl-CoA dehydrogenase apdG (Emericella nidulans (strain FGSC A4 / ATCC 38163 / CBS 112.46 / NRRL 194 / M139) OX=227321)"

Scaffold08_1726975	bioclim_12	0,968920595	maker-Scaffold08-exonerate_est2genome-gene-17.2/maker-Scaffold08-exonerate_est2genome-gene-17.2	"Similar to apdG: Acyl-CoA dehydrogenase apdG (Emericella nidulans (strain FGSC A4 / ATCC 38163 / CBS 112.46 / NRRL 194 / M139) OX=227321)"/"Similar to apdG: Acyl-CoA dehydrogenase apdG (Emericella nidulans (strain FGSC A4 / ATCC 38163 / CBS 112.46 / NRRL 194 / M139) OX=227321)"
Scaffold08_1728483	bioclim_12	0,968920595	maker-Scaffold08-exonerate_est2genome-gene-17.2/maker-Scaffold08-exonerate_est2genome-gene-17.2	"Similar to apdG: Acyl-CoA dehydrogenase apdG (Emericella nidulans (strain FGSC A4 / ATCC 38163 / CBS 112.46 / NRRL 194 / M139) OX=227321)"/"Similar to apdG: Acyl-CoA dehydrogenase apdG (Emericella nidulans (strain FGSC A4 / ATCC 38163 / CBS 112.46 / NRRL 194 / M139) OX=227321)"
Scaffold08_1728868	bioclim_12	0,968920595		
Scaffold08_1753670	bioclim_12	0,828248267	maker-Scaffold08-augustus-gene-17.35/maker-Scaffold08-augustus-gene-17.35	"Similar to CCDC174: Coiled-coil domain-containing protein 174 (Homo sapiens OX=9606)"/"Similar to CCDC174: Coiled-coil domain-containing protein 174 (Homo sapiens OX=9606)"
Scaffold08_2004441	bioclim_12	0,968920595	snap_masked-Scaffold08-abinit-gene-20.19/snap_masked-Scaffold08-abinit-gene-20.19	"Protein of unknown function"/"Protein of unknown function"
Scaffold08_2445418	bioclim_12	0,806497657	maker-Scaffold08-augustus-gene-24.52/maker-Scaffold08-augustus-gene-24.52	"Similar to MIMI_R883: Uncharacterized protein R883 (Acanthamoeba polyphaga mimivirus OX=212035)"/"Similar to MIMI_R883: Uncharacterized protein R883 (Acanthamoeba polyphaga mimivirus OX=212035)"
Scaffold08_2445443	bioclim_12	0,806497657	maker-Scaffold08-augustus-gene-24.52/maker-Scaffold08-augustus-gene-24.52	"Similar to MIMI_R883: Uncharacterized protein R883 (Acanthamoeba polyphaga mimivirus OX=212035)"/"Similar to MIMI_R883: Uncharacterized protein R883 (Acanthamoeba polyphaga mimivirus OX=212035)"

Scaffold08_2447210	bioclim_12	0,883816801	maker-Scaffold08-augustus-gene-24.52/maker-Scaffold08-augustus-gene-24.52	"Similar to MIMI_R883: Uncharacterized protein R883 (Acanthamoeba polyphaga mimivirus OX=212035)"/"Similar to MIMI_R883: Uncharacterized protein R883 (Acanthamoeba polyphaga mimivirus OX=212035)"
Scaffold08_2452149	bioclim_12	0,968920595		
Scaffold09_2286389	bioclim_12	0,867584111	maker-Scaffold09-augustus-gene-23.37	"Similar to ubc15: Ubiquitin-conjugating enzyme E2 15 (Schizosaccharomyces pombe (strain 972 / ATCC 24843) OX=284812)"
Scaffold09_2656056	bioclim_12	0,923108221		
Scaffold09_2690657	bioclim_12	0,892504127	snap_masked-Scaffold09-processed-gene-27.1	"Similar to CBH1: Exoglucanase 1 (Phanerochaete chrysosporium OX=5306)"
Scaffold11_971089	bioclim_12	0,883816801		
Scaffold11_973883	bioclim_12	0,883816801	maker-Scaffold11-snap-gene-9.27/maker-Scaffold11-snap-gene-9.27	"Similar to L3HYPDH: Trans-3-hydroxy-L-proline dehydratase (Homo sapiens OX=9606)"/"Similar to L3HYPDH: Trans-3-hydroxy-L-proline dehydratase (Homo sapiens OX=9606)"
Scaffold11_974171	bioclim_12	0,883816801	maker-Scaffold11-snap-gene-9.27/maker-Scaffold11-snap-gene-9.27	"Similar to L3HYPDH: Trans-3-hydroxy-L-proline dehydratase (Homo sapiens OX=9606)"/"Similar to L3HYPDH: Trans-3-hydroxy-L-proline dehydratase (Homo sapiens OX=9606)"
Scaffold11_974393	bioclim_12	0,883816801	maker-Scaffold11-snap-gene-9.27/maker-Scaffold11-snap-gene-9.27	"Similar to L3HYPDH: Trans-3-hydroxy-L-proline dehydratase (Homo sapiens OX=9606)"/"Similar to L3HYPDH: Trans-3-hydroxy-L-proline dehydratase (Homo sapiens OX=9606)"
Scaffold11_989832	bioclim_12	0,883816801	maker-Scaffold11-snap-gene-10.56/maker-Scaffold11-snap-gene-10.56	"Protein of unknown function"/"Protein of unknown function"
Scaffold11_991568	bioclim_12	0,883816801		
Scaffold11_992600	bioclim_12	0,883816801	maker-Scaffold11-snap-gene-10.36/maker-Scaffold11-snap-gene-10.36	"Similar to IML2: Inclusion body clearance protein IML2 (Coprinopsis cinerea (strain Okayama-7 / 130 / ATCC MYA-4618 / FGSC 9003) OX=240176)"/"Similar to IML2: Inclusion body clearance protein IML2 (Coprinopsis cinerea (strain Okayama-7 / 130 / ATCC MYA-4618 / FGSC 9003) OX=240176)"

Scaffold11_994658	bioclim_12	0,806497657	maker-Scaffold11-snap-gene-10.36/maker-Scaffold11-snap-gene-10.36	"Similar to IML2: Inclusion body clearance protein IML2 (Coprinopsis cinerea (strain Okayama-7 / 130 / ATCC MYA-4618 / FGSC 9003) OX=240176)"/"Similar to IML2: Inclusion body clearance protein IML2 (Coprinopsis cinerea (strain Okayama-7 / 130 / ATCC MYA-4618 / FGSC 9003) OX=240176)"
Scaffold11_997212	bioclim_12	0,892504127	maker-Scaffold11-snap-gene-10.57/maker-Scaffold11-snap-gene-10.36/maker-Scaffold11-snap-gene-10.57	
Scaffold11_999875	bioclim_12	0,892504127	maker-Scaffold11-snap-gene-10.36/maker-Scaffold11-snap-gene-10.36	"Similar to IML2: Inclusion body clearance protein IML2 (Coprinopsis cinerea (strain Okayama-7 / 130 / ATCC MYA-4618 / FGSC 9003) OX=240176)"/"Similar to IML2: Inclusion body clearance protein IML2 (Coprinopsis cinerea (strain Okayama-7 / 130 / ATCC MYA-4618 / FGSC 9003) OX=240176)"
Scaffold11_1075385	bioclim_12	0,892504127	maker-Scaffold11-snap-gene-10.69/maker-Scaffold11-snap-gene-10.69	"Protein of unknown function"/"Protein of unknown function"
Scaffold11_3597120	bioclim_12	0,86033947		
Scaffold11_3601220	bioclim_12	0,906371134		
Scaffold11_3608013	bioclim_12	0,906371134	genemark-Scaffold11-processed-gene-35.47/genemark-Scaffold11-processed-gene-35.47	"Similar to LAC: Laccase (Phlebia radiata OX=5308)"/"Similar to LAC: Laccase (Phlebia radiata OX=5308)"
Scaffold11_3615292	bioclim_12	0,906371134		
Scaffold11_3615344	bioclim_12	0,906371134		
Scaffold11_3616068	bioclim_12	0,906371134		
Scaffold11_3617356	bioclim_12	0,906371134		
Scaffold11_3617733	bioclim_12	0,828248267	maker-Scaffold11-exonerate_est2genome-	"Protein of unknown function"/"Protein of unknown function"

			gene-35.17/maker-Scaffold11-exonerate_est2genome-gene-35.17	
Scaffold11_3620095	bioclim_12	0,892504127	maker-Scaffold11-exonerate_protein2genome-gene-35.334/maker-Scaffold11-exonerate_protein2genome-gene-35.334	"Protein of unknown function"/"Protein of unknown function"
Scaffold11_3621201	bioclim_12	0,828248267	maker-Scaffold11-exonerate_protein2genome-gene-35.334/maker-Scaffold11-exonerate_protein2genome-gene-35.334	"Protein of unknown function"/"Protein of unknown function"
Scaffold12_1708900	bioclim_12	0,867584111	maker-Scaffold12-snap-gene-17.41/maker-Scaffold12-snap-gene-17.41	"Protein of unknown function"/"Protein of unknown function"